A Numerical Modelling Approach to Optimising Photovoltaic Installations for Thermal Effects Mitigation

Kudzanayi Chiteka (tavakudzira@gmail.com)
Harare Institute of Technology School of Engineering and Technology https://orcid.org/0000-0003-3697-5961

Luxmore Madiye
University of Zimbabwe

Hilton Chingosho
University of Zimbabwe

Rajesh Arora
Amity University Gurgaon

C.C Enweremadu
University of South Africa

Research Article

Keywords: Solar photovoltaics, thermal effects, thermal mitigation, modelling and simulation, optimisation

Posted Date: February 19th, 2021

DOI: https://doi.org/10.21203/rs.3.rs-242851/v1

A numerical modelling approach to optimising photovoltaic installations for thermal effects mitigation

K. Chiteka[1*], L. Madiye[2], H. Chingosho[2], R. Arora[3], C.C. Enweremadu[4]
[1]School of Engineering and Technology, Harare Institute of Technology, Harare, Zimbabwe.
[2]Department of Mechanical Engineering, University of Zimbabwe, Harare, Zimbabwe.
[3]Department of Mechanical Engineering, Amity University Haryana, Gurgaon-122413, India.
[4]Department of Mechanical and Industrial Engineering, University of South Africa, Florida, South Africa.
* Corresponding author, E-mail: tavakudzira@gmail.com

Abstract

Solar energy presents one of the best alternative sources of energy in the current bid to mitigate the negative impacts of global warming. The present study evaluated the influence of installation configuration together with the meteorological parameters on temperature characteristics of a solar photovoltaic array. Three dimensional simulation using Computational Fluid Dynamics was used in the numerical analysis of the temperature characteristics on solar PV arrays. The Shear Stress Transport k-ω model was employed to analyse the turbulent characteristics of the airstream near the photovoltaic array. A temperature prediction model was developed using Artificial Neural Networks and the model was found to be accurate with a coefficient of determination, R^2 above 90 %. A Response Surface Methodology optimization model was developed to maximize energy generation while minimizing solar photovoltaic cell operating temperature. The models were able to reduce temperature and improve energy generated by 3.9 %. The optimized tilt and azimuth angles were found to be 28.2^o tilt and 13.2^o respectively yielding an average cell temperature of 29.3 ^{o}C which gave 3.9 % increase in energy and revenue generated.

Keywords: Solar photovoltaics, thermal effects, thermal mitigation, modelling and simulation, optimisation.

List of Abbreviations

ABL	Atmospheric Boundary Layer	NNW	North of North West
ANNs	Artificial Neural Networks	NPV	Net Present Value
ANOVA	Analysis of Variance	PB	Pay Back
BIPV	Building Integrated Photovoltaics	PSO	Particle Swarm Optimisation
CCD	Central Composite Design	PV	Photovoltaic(s)
CFD	Computational Fluid Dynamics	PWAF	Present Worth Annuity Factor
CRF	Capital Recovery Factor	$PWAF_{es}$	Present Worth Annuity Factor (Escalated)
DI	Diffuse Irradiance	RANS	Reynolds Averaged Navier Stokes
DNI	Direct Normal Irradiance	RF	Random Forests
FVM	Finite Volume Method	RMSE	Residual Mean Square Error
GHI	Global Horizontal Irradiance	RSM	Response Surface Methodology
IR	Infrared Radiation	SIMPLE	Semi-implicit Method for Pressure Linked Equations
IRR	Internal Rate of Return	SOU	Second Order Upwind,
kWh	kilo-watt-hour	SST k-ω	Shear Stress Transport k-ω
MAPE	Mean Absolute Percentage Error	TKE	Turbulent Kinetic Energy
MWh	Mega-watt-hour	UDFs	User Defined Functions.
NASA	National Aeronautics and Space Administration	FiT	Feed - in - Tarriff
NNE	North of North East		

Introduction

Renewable energy sources have gained much traction in the last decade and can provide bulk of the global energy requirements. The issues to do with global warming and environmental degradation have necessitated the adoption of renewable energy sources particularly solar energy which is freely available in abundance (Kumar et al. 2014; Goel and Singh 2019a). As a result many countries have shifted their focus to clean and renewable energy sources (Goel and Singh 2019b). However, solar energy has its own shortcomings which include intermittency and its dependency on meteorological and environmental factors. There are three main factors affecting the performance of solar photovoltaics (PV) and these include irradiance, temperature and soiling (Lau et al. 2018).

The current PV technology is dominated by crystalline silicone modules contributing 90 % to the global PV market (Kumar and Rosen 2011). However, these are greatly affected by temperatures above 25 ^{o}C (Vafaei et al. 2015; Ahadi et al. 2016). Although heat gain is desirable in solar thermal systems (Goel and Singh 2017, 2020), it is definitely undesirable in solar PV systems. As the cell temperature increases, the PV array performance reduces considerably (Yadav and Bajpai 2018). In essence, there is a linear association between power loss and PV array temperature. Many correlations have been developed in studying the relationships between temperature and PV efficiency. For example, studies have indicated a performance loss between 0.1 %–0.65 %/K due to temperature (Kumar and Rosen 2011). This phenomenon justifies the importance of cooling in solar PV arrays mainly in hot climates (Zhang et al. 2017).

Cooling of solar PV collectors is indispensable in improving the power output in solar PV plants (Siecker et al. 2017). Some temperature mitigation procedures have been proposed and these include water cooling, use of hybrid systems (PV-Thermal), forced air circulation and natural air circulation (Wole-Osho et al. 2020). Wind or air flow plays a significant role in lowering the array temperature thus improving the performance of the PV array. Mirzaei and Carmeliet (2015) evaluated the simultaneous airflow both underneath and above the PV modules to assess the temperature characteristics on the PV array using infrared thermography. It was noted that there was non-uniform distribution of surface temperature owing to the lateral eddies developed in the flow. In a different study, the role of cavity airflow on PV array performance was investigated using particle image velocimetry and it was found that the upstream velocity can be 1.26 to 1.35 times slower than the airflow in the cavity (Mirzaei et al. 2014). The results also indicated that turbulent mixing in a stepped configuration of PV modules yields better performance compared to a flat configuration. Studies have also shown that, air flow both in form of forced convection or natural convection has a cooling effect on the solar PV module (Goossens et al. 2019), thus wind-driven temperature mitigation is therefore widely accepted (Zhang et al. 2017). Al-Nimr et al. (2018) proposed a hybrid wind/PV system to minimise temperature rise on the PV cells through the use of a wind turbine. It was shown that through this hybrid system, more energy was generated by both the wind turbine and the PV system.

Incorporating the major parameters influencing PV performance in optimising the installation configuration is of great importance. The effects of irradiance and temperature on PV performance have been widely studied (Kumar et al. 2020). However, these studies mainly concentrated on analysing the effects of these parameters on PV performance (Dubey et al. 2013). Many studies have only highlighted the importance of irradiance on optimisation of the installation configuration. Some studies have proposed the incorporation of other parameters such as soiling and shading in the optimisation of the installation configuration (Lau et al. 2018). However, the effect of temperature has not been fully investigated. Attempts have been made to evaluate the effects of cooling on PV array performance, and it was reported that increasing wind speeds improves the PV array performance (Kaldellis et al. 2014).

Under normal circumstances factors which include wind speed and direction have a substantial contribution on the PV cell temperature although its analysis is complex due to the stochastic nature of wind. However, if the cooling effect of wind is taken into consideration, the optimum installation configuration can be different from the generally accepted configuration. The optimisation of

installation configuration to utilise the cooling effect of wind is still yet to be investigated. Previous studies were mainly concerned with wind flow cooling effect on solar photovoltaics (PV) systems. The optimisation of such systems to maximise power generation while minimising the thermal effects has not been widely considered. The generally accepted optimum PV installation configuration only take the solar irradiance into consideration. The influence of other important factors such as temperature and the possible mitigation approaches for maximum energy yield have been generally overlooked. In optimisation of PV array installation configuration, there is need to consider other factors such as temperature effects. Although it is a complex approach, this will lead to a better optimisation model and higher energy yields. If installations are optimised, higher energy yields are obtained and this improves the revenues generated. This study therefore focuses on developing a predictive model for PV array temperature and establish an optimisation model to minimise temperature effects while maximising energy yield. The study is based on the premise that, of the major parameters influencing solar energy yield, i.e. irradiance, temperature and soiling, irradiance has been widely investigated and installation optimisation has been studied based on irradiance. However, temperature is also an important factor which need to be considered in determining optimal installation configuration.
This research study is organised as follows; section 1 introduces the issues of thermal effects on PV performance. The related literature is also scanned in light of the present study. Section 2 presents the research approaches and methods used in this study. These include the experimental setup, the simulation approaches and techniques used. The data collection and validation mechanisms used are also discussed in this section. Section 3 outlines and discusses the results obtained from the simulation analysis. The techno-economic and optimisation analysis of the present study is also considered in this section leading to the conclusions in Section 4.

Materials and Methods

The initial step involved feature extraction from a wide array of meteorological parameters which was done to select the best parameters for predictive modelling and simulation. This was followed by the development of a temperature predictive model using selected meteorological parameters. The third step involved simulations on solar energy generated under varying tilt and azimuth (also known as orientation) angles. Having ascertained the implications on energy of varying the tilt and orientation, experimental design was performed to determine the minimum number of simulations that can be run in CFD. The simulations were run and on each simulation the average and maximum cell temperature were recorded and this was used to determine the thermal losses for each simulated configuration. These thermal losses were used as input in PVSyst for energy simulations. This was followed by optimisation for both temperature minimisation and energy maximisation. Finally, to determine the effectiveness of the optimisation model in financial terms, and economic analysis was done.

Parameter correlation and dimensionality reduction

Parameter correlation was performed to establish the relationships between the different meteorological parameters with temperature. Fourteen environmental and meteorological parameters were obtained from "NASA Solar Energy and Surface Meteorology" for use in temperature prediction and optimisation modelling. The meteorological parameters used are; precipitation (R), surface pressure (P), relative humidity (H), Diffuse Irradiance (DI), Global Horizontal Irradiance (GHI), Direct Normal Irradiance (DNI), minimum wind speed (W_{min}), maximum wind speed (W_{max}), wind speed (W_s), wind direction (W_d), wind speed range (W_{range}), average temperature (T_{avg}), clearness index (C) and Downward Thermal Infrared radiative flux (IR). Software python v3.8 was used and these meteorological parameters were used in parameter correlation. Average temperature was taken as the response variable and the other parameters were used as the predictor variables. Selection of all relevant parameters was accomplished using Boruta algorithm in

Python software. The selected parameters were used in developing the prediction model in Artificial Neural Networks (ANNs).

Artificial Neural Networks (ANNs) model

An Artificial Neural Network model was developed to establish the association between meteorological parameters against the ambient temperature which can be used to predict the temperature of PV collectors. Literature reveals that ANNs have been successfully used in situations where there is difficulty in establishing the relationship between the predictor and predicted variables both analytically and mathematically (Conceição et al. 2018).

In this study, a feed forward backpropagation neural network was trained using the Levenberg-Marquardt algorithm. This training algorithm was selected due to its high computational speed notwithstanding that it also demands huge memory resources. The gradient descent learning algorithm with momentum was selected with input variables taken from the all-important variables obtained from the Boruta algorithm. All the values used in this study were normalised between the range 0 - 1 as shown by Equation 1. Original non-normalised values were obtained by employing Equation 2.

$$V_n = \frac{V - V_{\min}}{V_{\max} - V_{\min}} \quad (1)$$

$$V_p = V_n \left(V_{\max} - V_{\min}\right) + V_{\min} \quad (2)$$

Where: V_n is the normalised value, V_{min} is the minimum measured value, V_{max} is the measured maximum value while V_p is the value predicted by the ANN model.

All the relevant features obtained from Boruta algorithm were used as input parameters. The ANN had a single hidden layer having neurons which were varied between 10 and 50 with a step of five. The ANN also had a single output layer with temperature as the target value. Selection of the best performing combination of activation functions for both the hidden and output layer was done. All the different combinations of two of the three assessed activation functions were analysed for their performance in an ANN with a fixed number neurons equal to 25. The transfer functions evaluated were pure linear (purelin), hyperbolic tangent sigmoid (tansig) and logistic sigmoid (losig).

One combination of transfer functions was used to select the best number of neurons to be used in the modelling process. There was random initialisation of the weights used in model development. A ratio of 70:15:15 was used to assign data respectively for training, testing and validation. 3652 data sets obtained from NASA for the period 2009 to 2019, was thus split for training, testing and validation with respective number of datasets given by 2556, 548 and 548. The ANN toolbox in in MATLAB® release R2018a was used in the modelling process.

Experimental design

Different variations of the installation configurations to analyse their effect on array temperature were obtained using face centred, central composite design of experiments implemented using Design Expert software v12.0 with a layout shown in Table 1. The parameters used in the experimental design are tilt, orientation and, wind speed and direction. Tilt angles were varied from 8° to 38° and the installation orientation (azimuth) had values varying from -22.5° (North of North West, NNW) to 22.5° (North of North East, NNE).

The wind direction and speed assumed values obtained from NASA through the use of User Defined Functions (UDFs). The results obtained from the CFD simulations with varying

installation parameters were used to generate a response surface for mapping the relationship between installation parameters, temperature and energy generated by a solar PV module.

Table 1. Experimental design.

	Factor 1	Factor 2	Factor 3	Factor 4
Run	A:Tilt (°)	B:Orientation (°)	Wind speed (m/s)	Wind direction (°)
1	23	0	10 year (2009 – 2019) hourly data file obtained from NASA	
2	23	-22.5		
3	8	0		
4	38	-22.5		
5	8	-22.5		
6	38	22.5		
7	23	0		
8	23	0		
9	23	22.5		
10	38	0		
11	8	22.5		
12	23	0		
13	23	0		

Simulations using Computational Fluid Dynamics (CFD)

The Reynolds Averaged Navier Stokes (RANS) governing Equations represented by Equation 3 were used to model the air flow around the PV array. The turbulence model, SST k-ω shown by Equation 4 - 5 was adopted to compute the turbulent behaviour of the flowing fluid air.

$$\rho\frac{\partial\bar{\varnothing}}{\partial t}+\rho\bar{u}_j\frac{\partial\bar{\varnothing}}{\partial x_j}-\frac{\partial}{\partial x_j}\left[\Gamma_{\varnothing,\text{eff}}\frac{\partial\bar{\varnothing}}{\partial x_j}\right]=S_{\varnothing} \quad (3)$$

Where; ρ (kg/m^3) is the density, while time taken is t (seconds) and the velocity vector is **u** (m/s). κ (W/mK) is the thermal conductivity and the independent flow variable is $\emptyset$. $\Gamma_{\emptyset,\text{eff}}$ (m^2/s) represents the effective diffusion coefficient while $S_{\emptyset}$ is the source term.

$$\frac{\partial}{\partial t}(\rho k)+\frac{\partial}{\partial x_i}(\rho k u_i)=\frac{\partial}{\partial x_j}\left(\xi_k\frac{\partial k}{\partial x_j}\right)+g_k-y_k+s_k \quad (4)$$

$$\frac{\partial}{\partial t}(\rho\omega)+\frac{\partial}{\partial x_i}(\rho\omega u_i)=\frac{\partial}{\partial x_j}\left(\xi_\omega\frac{\partial\omega}{\partial x_j}\right)+g_\omega-y_\omega+d_\omega+s_\omega \quad (5)$$

Where; g_k is the turbulent kinetic energy generation term; g_ω is the specific dissipation rate generation term; ξ_ω and ξ_k are respectively the effective diffusivity of ω and k. The dissipation rates of k and ω are respectively given by y_k and y_ω; The cross diffusion term is given by d_ω; The user defined source terms taken as zero in this study are represented by s_k and s_ω.

The geometry used in the simulation was developed using ANSYS design Modeller v17.0 and it mimicked the geometry used by Abiola-Ogedengbe (2011) in his wind tunnel experiments. The

ground mounted PV array had its tilt and orientation respectively varied from 8° to 38° and -22.5° to 22.5° while its height of installation h_p was 1.5m. The UDFs (file) were used to provide the values of wind speed and wind direction. Respective dimensions of 21.4 h_p, 6 h_p and 9 h_p were used for the length, height and width of the computational domain. $5h_p$ and $15h_p$ were respectively the distances from the inlet to the PV array and from the PV array to the outlet of the computational domain. These dimensions guaranteed no obstruction of air flow on the PV array surface.
A mesh of structured grids was developed using ANSYS ICEM 17. This mesh had 600 000 nodes and was adopted after a mesh independence study. The Finite Volume Method (FVM) was adopted in resolving wind flow conservation equations. Pressure and velocity flow fields were decoupled by employing the SIMPLE algorithm. Diffusion and convection terms were discretised by making use of the second-order upwind scheme represented by Equation 6 (ANSYS FLUENT GUIDE 2013).

$$\gamma_{f,sou} = \gamma + \gamma_{grad}.\vec{\mathrm{r}} \qquad (6)$$

Where; the face value using second order upwind is given by $\gamma_{f,sou}$; The cell-centred value γ had its gradient γ_{grad} in the cell upstream; The displacement vector $\vec{\mathrm{r}}$ is measured from the face centroid to upstream cell centroid. Simulations were done to compute airflow fields on the PV module. The pressure coefficient, C_p profile obtained in the simulations was validated against the pressure coefficient profile obtained by Tominaga et al. (2015). The C_p from simulations had a percentage difference of 1.03% with the C_p from experimental studies and hence the simulation model was concluded to be able to precisely compute the airflow fields around the PV collector.

Thermal Losses, temperature and radiation modelling

The solar ray tracing model was used for the selected location (Harare). Radiation flux was obtained from the Stefan-Boltzmann relationship given by Equation 7 where the Stefan-Boltzmann constant, $\sigma = 5.67\mathrm{x}10^{-8}$. A_s is the surface area, ε is the emissivity (assumed to be 1), T_p is the temperature of the sun while T_s is the temperature of the surroundings.

$$q = A_s \varepsilon \sigma \left(T_p^4 - T_s^4\right) \qquad (7)$$

The thermal losses incorporated in PVsyst were determined using the relationship shown by Equation 8; Where, U is the thermal behaviour, T_c is the temperature of the solar cell, T_a is the ambient temperature, α is the absorption coefficient, H is the global horizontal irradiance while η is the PV cell efficiency.

$$U\left(T_c - T_a\right) = \alpha H\left(1 - \eta\right) \qquad (8)$$

Optimisation

The CFD simulation results were used to determine the optimum configuration for minimising temperature while maximising energy generated. Response Surface Methodology (RSM) was employed to generate a 2nd order polynomial modelling the relationship between installation configurations, temperature and energy. The resulting temperatures from different simulations were used to simulate energy production using PVSyst for a full year. An empirical model (Equation 9) was used for predicting solar radiation availability on a tilted PV module surface. This radiation on a tilted PV module, I_t is obtained from the Global Horizontal Irradiance (GHI) which is obtained from Reflected Irradiance (I_r), Diffuse Irradiance and (I_d) Beam Irradiance (I_b), where; r_b, r_r and r_d are tilt factors for beam, reflected and diffuse irradiance.

$$I_t = I_b r_b + I_d r_d + (I_b + I_d) r_r \quad (9)$$

Results and discussions

Solar radiation and energy generated

The collectors were facing the general north direction i.e. North of North West (NNW), North (N) and North of North East (NNE) to harvest as much energy as possible. The different combinations of tilt (from 5° to 44°) and orientation (from -22.5° to 22.5°) were assessed. The simulations revealed that the maximum possible annual energy loss obtained after varying the parameters within the specified range was 5.1% as shown in Table 2 and 3. However, the range between 8° and 38° was chosen for optimisation in this study and the maximum energy loss within this range was found to be 2.5% which is reasonably low. This range was chosen based on the generally accepted deviation in tilt angle of φ ± 15° where φ is the latitude of the location (Hartner et al. 2015).

Table 2. Energy generated and losses for each configuration

	Factor		Response	
Run	B:Orientation (°)	A:Tilt (°)	Annual energy (kWh/m²)	Energy loss (%)
1	0	5	1947	2.90
2	0	8	1971	1.70
3	0	11	1991	0.70
4	0	14	2007	0.00
5	0	17	2018	0.00
6	0	20	2024	0.00
7	0	23	2026	0.00
8	0	26	2024	0.00
9	0	29	2017	0.00
10	0	32	2006	0.00
11	0	35	1991	0.70
12	0	38	1972	1.70
13	0	41	1948	2.90
14	0	44	1920	4.30
15	-22.5	5	1944	3.10
16	-22.5	8	1966	1.90
17	-22.5	11	1984	1.00
18	-22.5	14	1997	0.40
19	-22.5	17	2007	0.00
20	-22.5	20	2013	0.00
21	-22.5	23	2014	0.00
22	-22.5	26	2011	0.00
23	-22.5	29	2004	0.00
24	-22.5	32	1993	0.60
25	-22.5	35	1978	1.30

26	-22.5	38	1959	2.30
27	-22.5	41	1937	3.40
28	-22.5	44	1909	4.80
29	22.5	5	1943	3.10
30	22.5	8	1965	2.00
31	22.5	11	1983	1.10
32	22.5	14	1996	0.50
33	22.5	17	2005	0.00
34	22.5	20	2011	0.00
35	22.5	23	2012	0.00
36	22.5	26	2008	0.00
37	22.5	29	2001	0.20
38	22.5	32	1990	0.80
39	22.5	35	1975	1.50
40	22.5	38	1955	2.50
41	22.5	41	1934	3.70
42	22.5	44	1893	5.10

Table 3. Transposition factors and maximum possible annual energy yield at tilt angle of 23°

	NNW	N	NNE
Transposition factor	1.06	1.07	1.06
Annual energy generated (MWh)	49.0	49.6	49.6
% difference of annual energy yield	1.8%	0%	0%
% difference of transposition factor	0.93%	0%	0.93%

The variation of energy generated with the tilt angle was modelled using a quadratic function as shown by Equations 10 – 12 respectively for 0°, -22.5° and 22.5° azimuth angles where y is the energy generated and x is the tilt angle.

$$y = 1897.278 + 11.18374x - 0.2426743x^2 \quad (10)$$

$$y = 1897.815 + 10.30106x - 0.2284464x^2 \quad (11)$$

$$y = 1897.601 + 10.21734x - 0.2286441x^2 \quad (12)$$

It was found that when the orientation is facing due west, there is slightly more energy generated compared to orientations due east. It is also revealed that the variation of energy generated with respect to tilt angle can be modelled using a quadratic polynomial.

Parameter correlation analysis and selection of controllable parameters

Parameter correlation was performed in random forests applying the Boruta algorithm. The RandomizedSearchCV obtained from sklearn was used to optimise the hyper parameters. Four variables were selected by the algorithm and these were pressure, humidity, wind speed and wind direction. These parameters were selected with a test accuracy of 96.4%. The parameter selection indicate that wind direction, wind speed, humidity and pressure are closely correlated to ambient

temperature. However, of these parameters, two are controllable and the other two are not controllable. Wind speed and direction are controllable parameters on installation configuration while pressure and humidity are non-controllable and hence cannot be used for temperature mitigation. However, these parameters are essential in predictive modelling of ambient temperature (See Fig. 1).

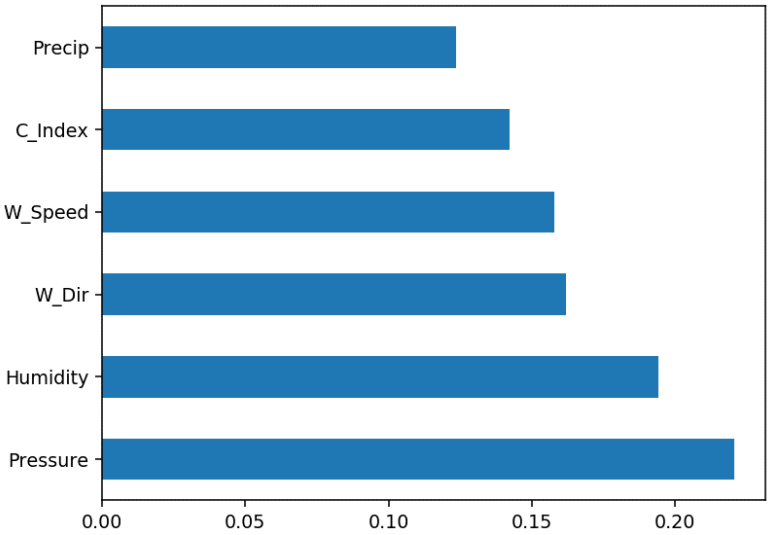

Fig. 1. Parameter correlation analysis using Boruta algorithm.

The correlation matrix used for variable selection shows that pressure has a very strong correlation with temperature. Other factors of influence include precipitation and clearness index as shown in Fig. 2. The relationship between pressure, relative humidity, wind speed and wind direction was analysed and the graphs are shown in Fig. 3.
The correlation of each of the selected variables with temperature was analysed using regression analysis. As shown in Fig. 3. The coefficients of determination R^2 values of relative humidity, pressure, wind direction and wind speed are respectively 50.92%, 17.24%, 12.04% and 25.21%. The individual correlations show that relative humidity has the strongest correlation with temperature followed by wind speed.

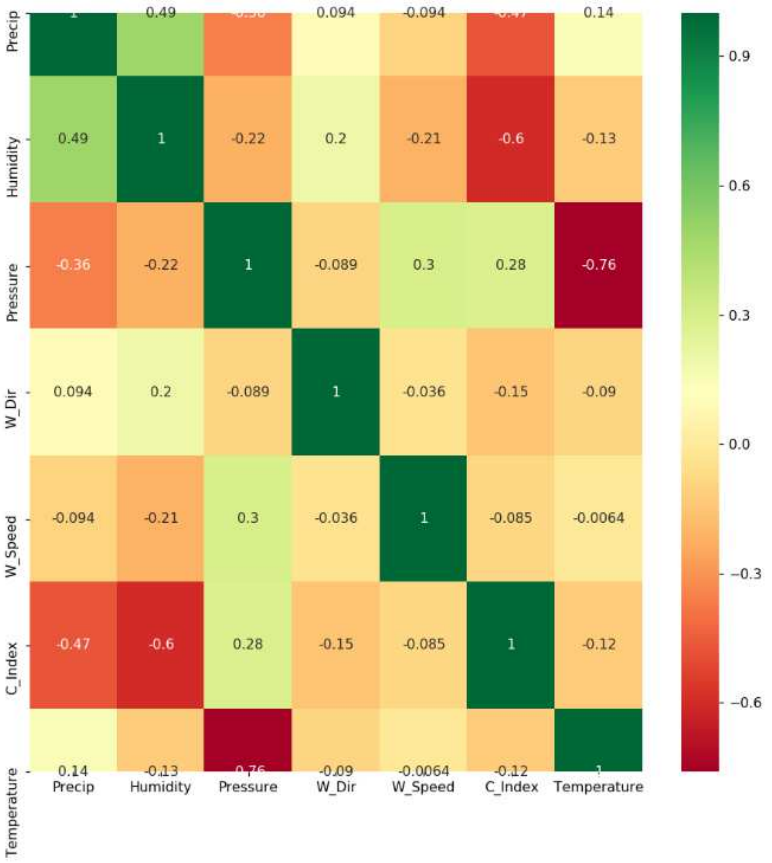

Fig. 2. Correlation matrix for variable selection

From the parameter correlation analysis, some controllable parameters were selected. It was shown that the maximum and average wind speeds are respectively 9.22 m/s and 3.56 m/s. (See Fig. 4). The general wind direction is from the East especially from ENE to NNE. Such a phenomenon will make the collector facing NNE have more direct interactions with the wind while the NNW configuration has less direct interactions with the wind thereby experiencing less temperature reduction.

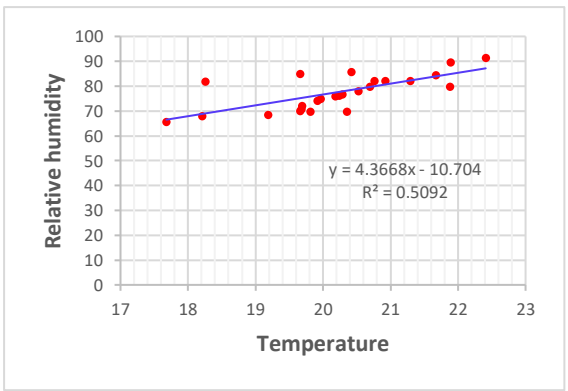

(a)

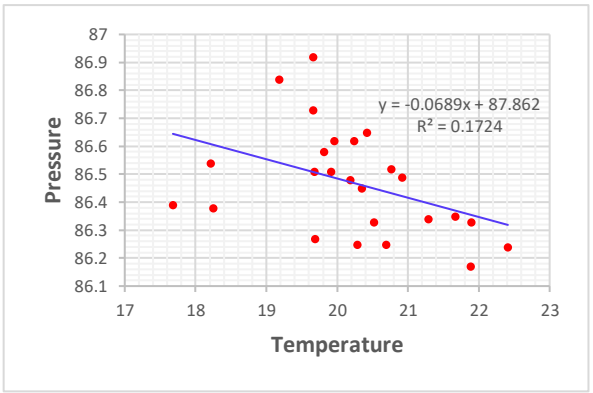

(b)

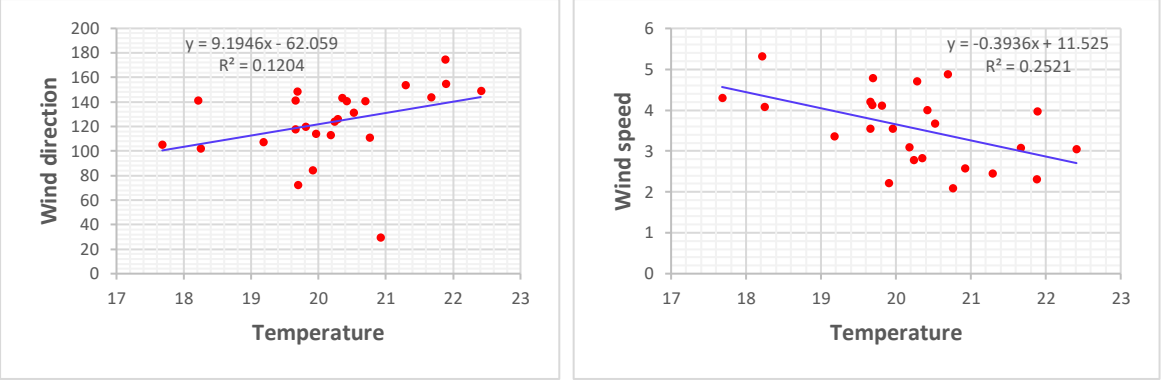

(c) (d)

Fig. 3. Correlation of temperature with; relative humidity (a), pressure (b), wind direction (c) and wind speed (d).

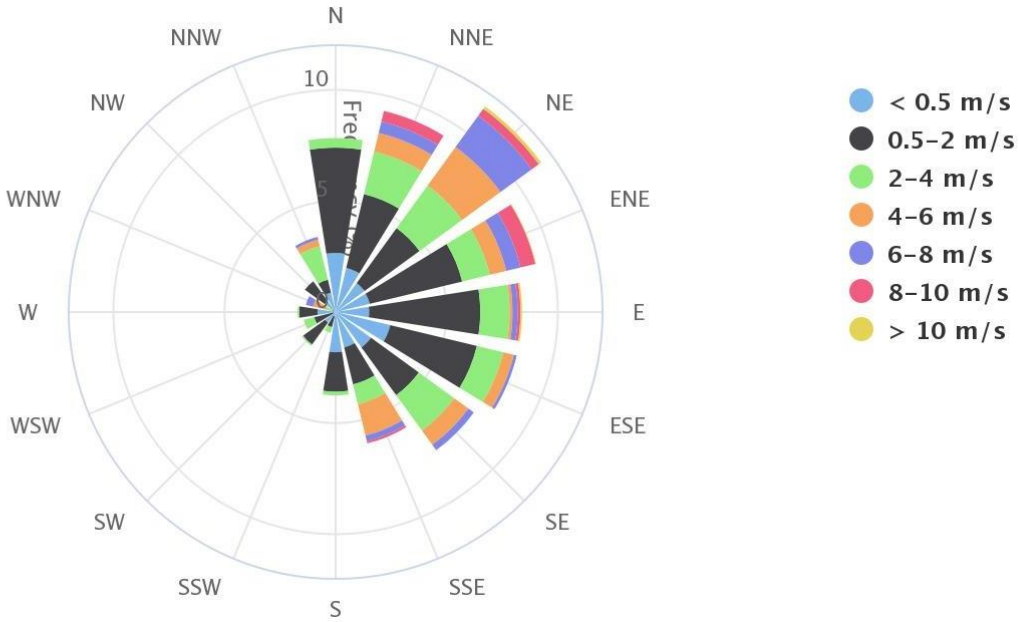

Fig. 4. Wind Rose showing the 10 year annual average wind speed and direction

Temperature prediction model

An ANN prediction model was developed and run in Matlab 2018a. The assessment of activation functions revealed that the Logistic Sigmoid transfer function in the hidden layer and the pure linear activation function in the output layer performed the best for all combinations of activation functions evaluated in this study (See Table 4). A total of 35 neurons were selected and used in the model as they gave the best results and this is outlined in Table 5.

Table 4. Analysis of activation functions

	Activation Functions		Accuracy (R^2) (%)
	Hidden Layer	Output Layer	
1	Logsig	Logsig	69.85
2	Logsig	Tansig	72.31
3	Logsig	Purelin	90.85
4	Tansig	Logsig	53.26

5	Tansig	Tansig	66.89
6	Tansig	Purelin	81.69
7	Purelin	Logsig	51.03
8	Purelin	Tansig	55.36
9	Purelin	Purelin	48.64

Table 5. Selection of number of neurons

	Number of neurons	**Accuracy (R^2) (%)**
1	10	72.56
2	15	75.68
3	20	86.91
4	25	87.82
5	30	90.23
6	35	90.85
7	40	90.85
8	45	90.86
9	50	90.86

The ANN model was developed in Matlab and was found to perform well with R^2 values above 90%. Fig. 5 reveals the performance validation of the developed ANN model. The predicted values of ambient temperature were compared to the expected values and the model was found to have a coefficient of determination of 90.85%.

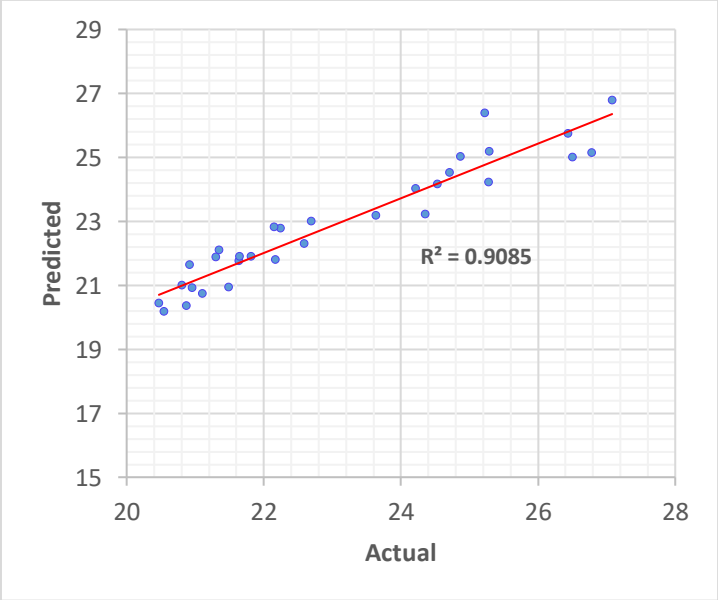

Fig. 5. ANN model validation

CFD simulation results

Profiles of air flow velocity

The wind flow characteristics around the PV module were used to deduce the rate of heating of solar PV modules with varying installation configurations (Fig. 6). The results show some complex airflow velocity fields around the solar collector and this results from the presence of the solar PV

array as a wind barrier thus hindering free flow of wind. This occurrence was also reported in a study by Lu and Zhao (2019).

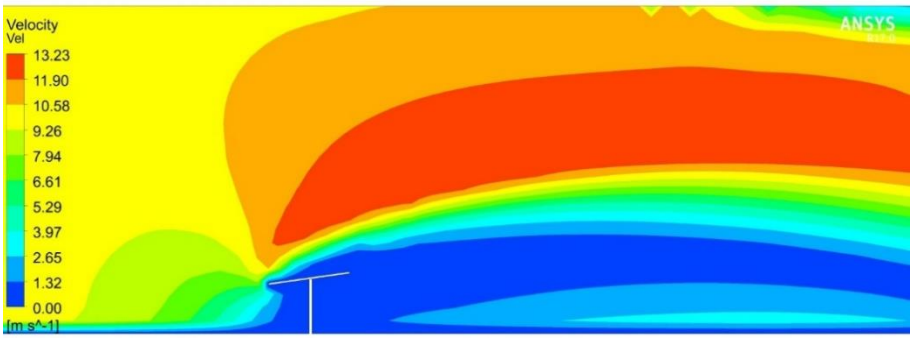

(a) 8° tilt

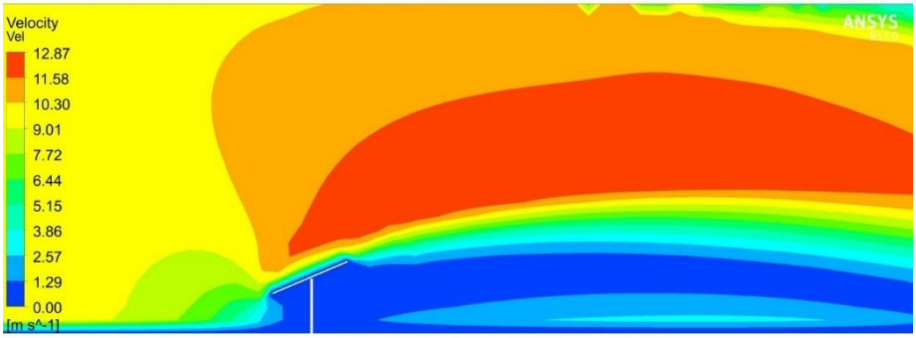

(b) 23° tilt

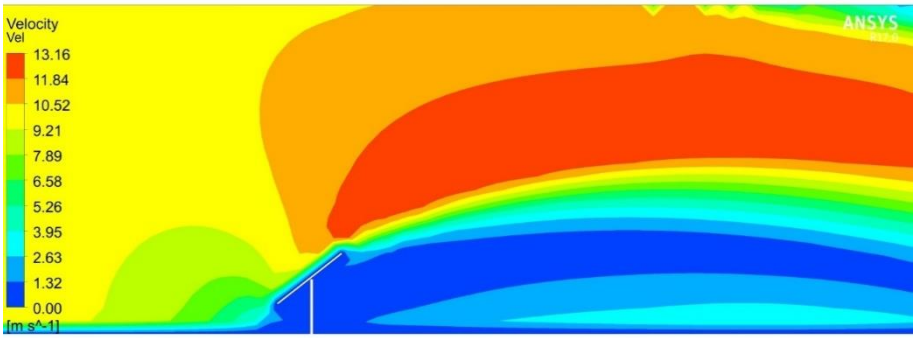

(c) 38° tilt

Fig. 6. Velocity profiles

The velocity fields are different for different tilt angles with less obstructions occurring at lower tilt angles and higher obstructions being recorded on steeper tilt angles. Steeper tilt angles resulted in more wind-PV interactions thus causing more cooling in steeper tilt angles compared to less steep tilt angles. This was as a result of a larger effective surface area exposed to the flowing wind by steeper tilt angles. Lower impact wind velocities were recorded on lower tilt angles compared to the steeper tilt angles. An average of 9.99 m/s impact velocity was experienced on the 8° tilt angle configuration against an average impact velocity of 10.03 m/s for steeper tilt angles. This is the reason for more cooling occuring on higher tilt angles while less cooling occurs on lower tilt angles. Both average temperatures (T_{avg}) and maximum temperatures (T_{max}) were found to be increasingly lower with increasing tilt angle.

TKE profiles

The results indicate that higher tilt angles cause higher turbulences and hence TKE values increased with increasing tilt angles. As shown in Fig. 7, the results gave average TKE values of 0.264 m^2/s^2, 0.316 m^2/s^2 and 0.395 m^2/s^2 respectively for 8°, 23°, and 38°. Higher turbulences experienced on higher tilt angles are the reason for the lower temperatures experienced on steeper tilt angles compared to lower tilt angles. This is because higher wind turbulences have a tendency of dissipating the heat generated on the PV collector.

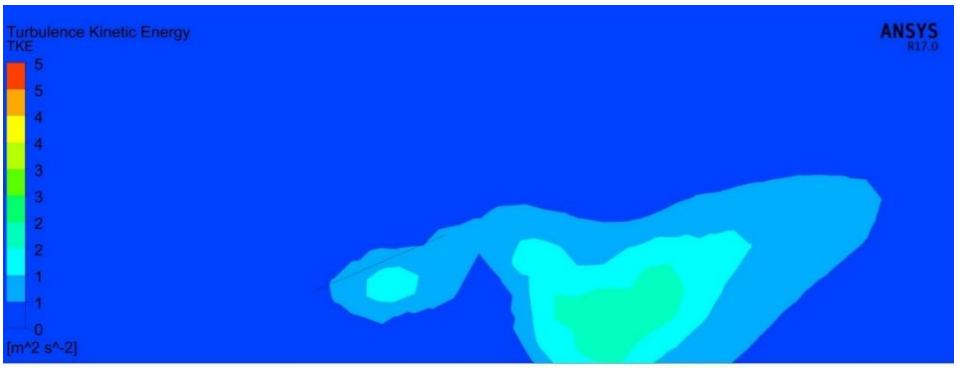

(a)

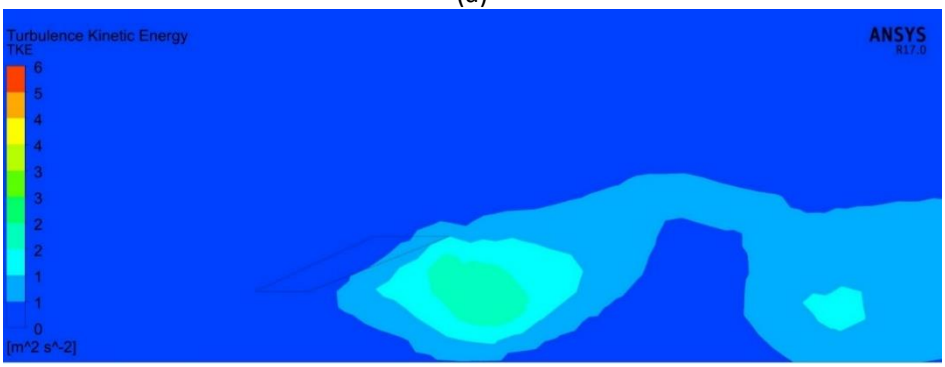

(b)

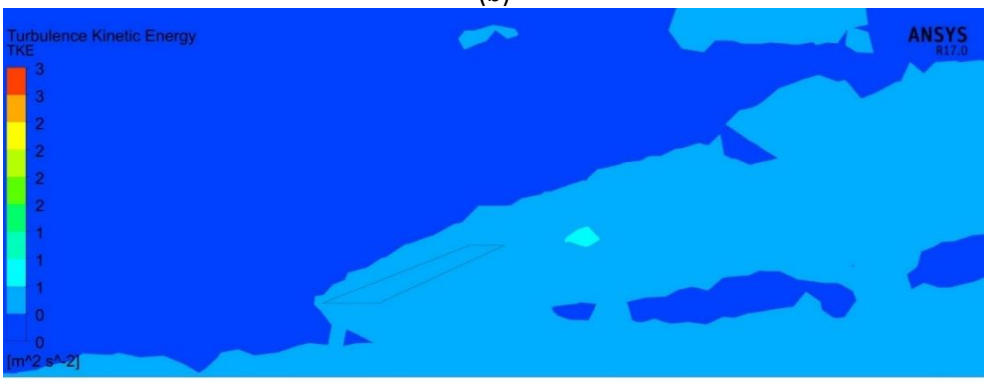

(c)

Fig. 7. TKE Profiles at 23° tilt; (a) 0° orientation, (b) 22.5° orientation, (c) -22.5° orientation

The orientation of installation also shows its importance in the cooling of the solar PV arrays as evident from the 22.5° (Fig. 8) configuration which shows higher turbulences compared to other configurations. This is expected since more wind flow was expected in that direction compared to other directions.

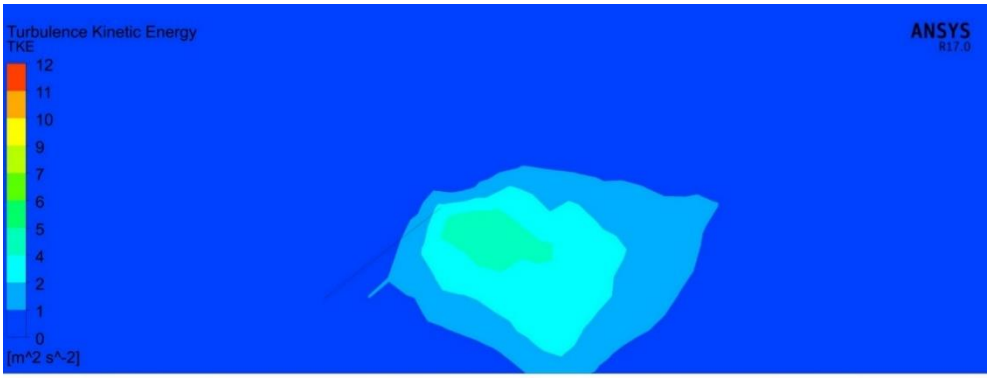

(a)

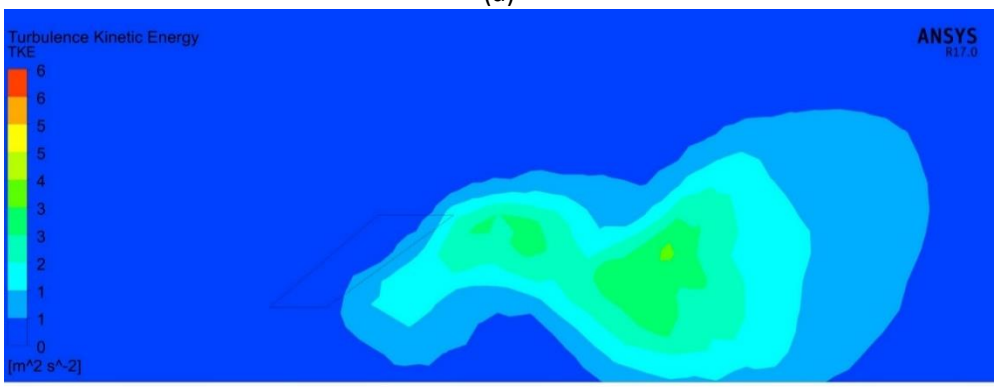

(b)

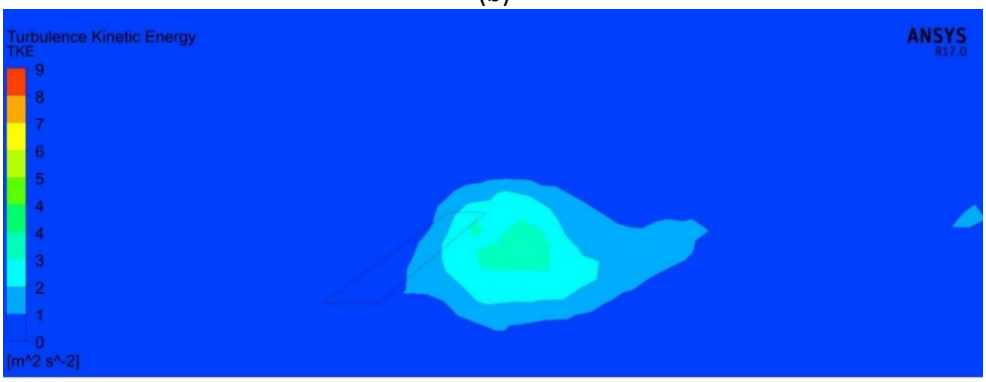

(c)

Fig. 8. TKE Profiles at 38° tilt; (a) 0° orientation, (b) 22.5° orientation, (c) -22.5° orientation

Temperature Profiles

The simulations in this study used JA Solar PV module. In this case T_{NOCT} was taken as 45 °C. The results were validated against the established relationship (Equation 13) to calculate the cell temperature given the ambient temperature. There was only a 0.28 % average prediction error in the CFD model when compared to the results obtained from Equation 19. The results obtained in the CFD simulations indicate a 5 % increase in average temperature for 8° tilt and a 3 % average decrease in temperature for 38° tilt angle when both are compared to the 23° tilt angle.

$$T_c = T_a + (T_{NOCT} - 20)\frac{G}{800} \quad (13)$$

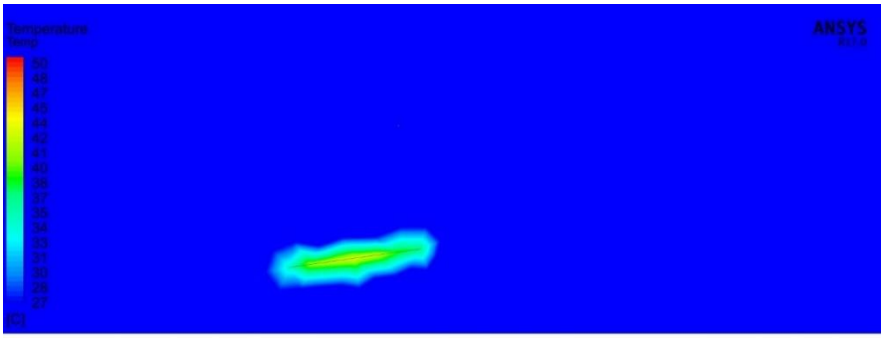

(a)

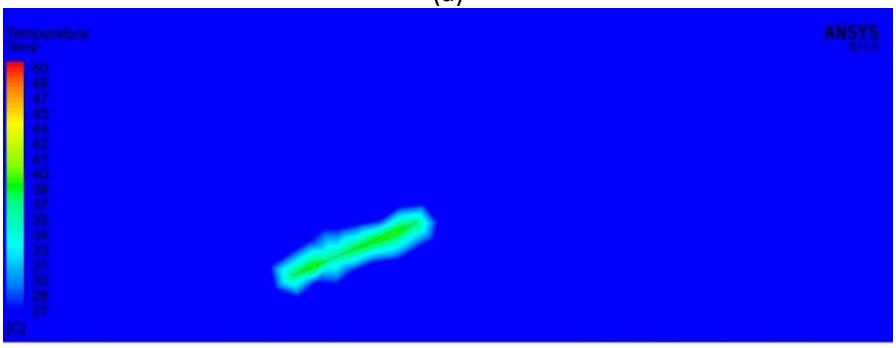

(b)

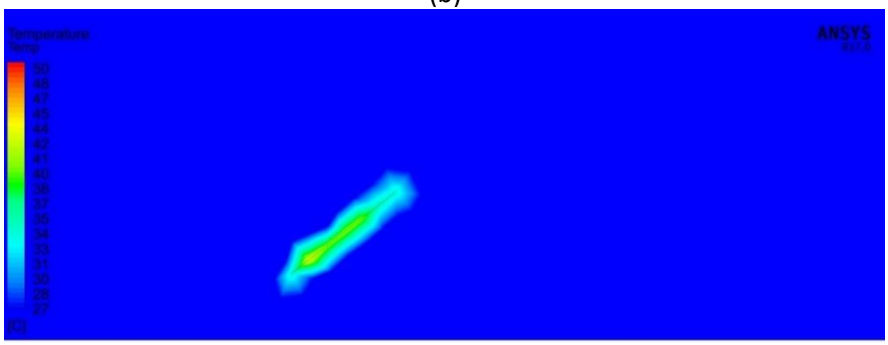

(c)

Fig. 9. Temperature profiles at 0° orientation; (a) 8° tilt, (b) 23° tilt (c) 38° tilt

From Fig. 9, the PV module temperature profiles are shown and the profiles indicate that more heating was experienced on the 8° tilt followed by 23° and then 38° tilt angles. The profiles reveal that the temperatures experienced on the solar PV module are well above the ambient temperatures for all configurations. These high temperatures result in energy losses.

Velocity streamlines

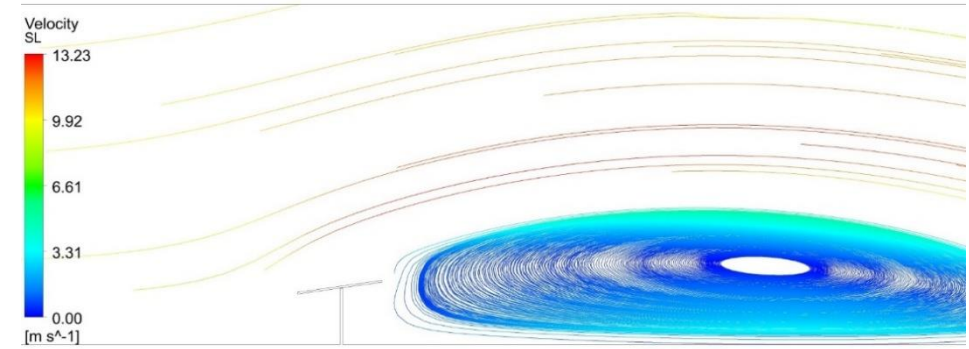

(a)

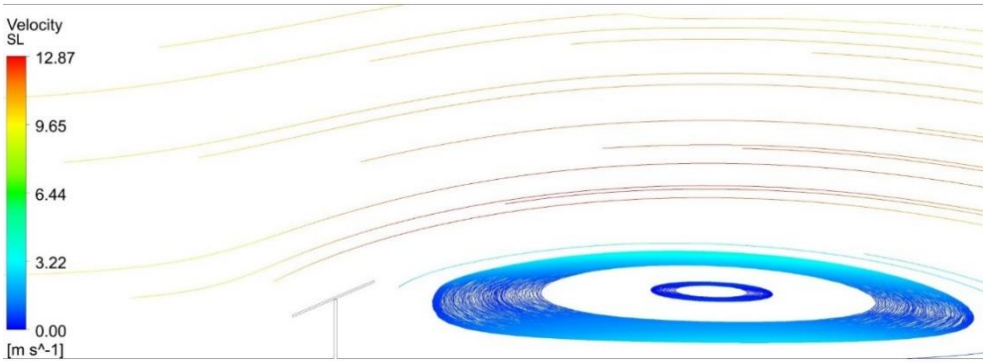

(b)

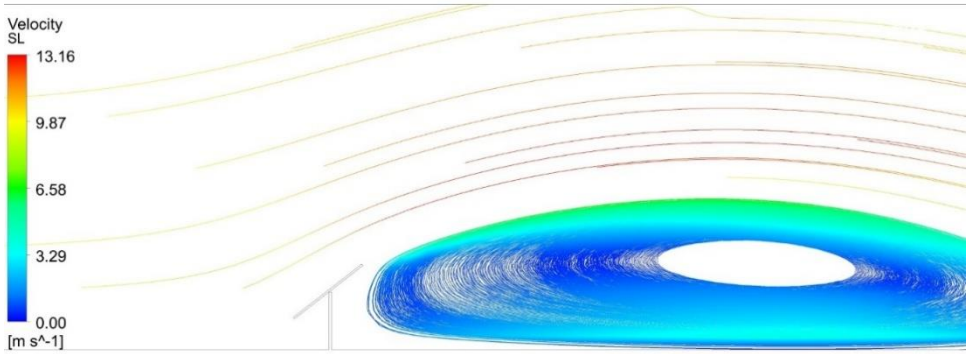

(c)

Fig. 10. Velocity streamlines at tilt degrees of (a) 8° (b) 23° and (c) 38°

Air flow velocity streamlines around the solar PV collector are shown in Fig. 10. These streamlines characterise the path followed by fluid air particles and they describe flow in terms of velocity and direction. The flow velocity and the spacing between the streamlines are inversely proportional to each other.

There are turbulent eddies behind the PV module for all configurations. These turbulent eddies were much closer to the PV module for the 38° tilt and this had an effect of causing more cooling compared to the other tilt angles.

Response surface modelling

The values of average solar PV module temperature, maximum PV module temperature reached, TKE and average velocity were obtained from the simulations. Response Surface Methodology (RSM) was used to analyse these results and models were developed from these results.

Temperature as the most important output variable was analysed against the installation variables used in this study. The results revealed that the tilt angle and the orientation had a strong relationship with PV module temperature. The simulation results were used to generate contours

and response surfaces shown in Fig. 11 and the analysis of the contours generated was performed. The analysis of both the contours and the response surface revealed that both the tilt and the azimuth angle of installation had a significant contribution to the PV module temperature. It is evident that at the minimum azimuth of -22.5° and a tilt of 8° there is maximum temperature generation. This is validated by the fact that the wind direction in this study was found to be mainly concentrated on the eastern direction and hence more cooling was expected in the eastern orientation compared to the western orientation. The minimum temperatures were attained at an orientation of 22.5° and tilt of 38° with temperatures in the range of 30°. Also a tilt of 8° at an orientation of 22.5° gave a temperatures around 50 °C experienced in this simulation. Tilt angles from 20° to 38° at orientations between 0° and 22.5° gave cell temperatures of 40 °C and below.

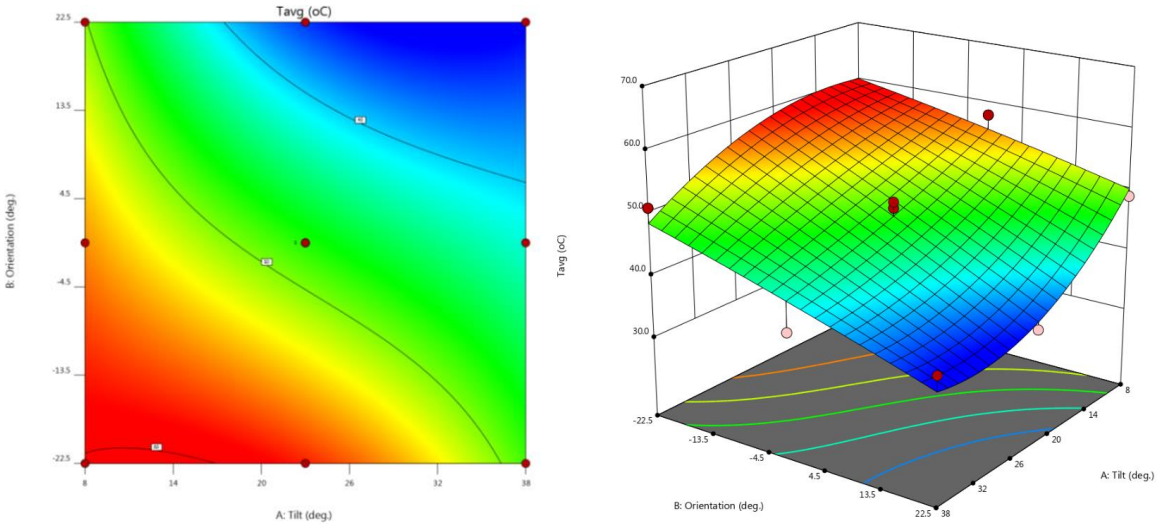

(a) (b)

Fig. 11. Average temperature contours Response surface for the average temperature.

Numerical optimization and economic analysis

Minimising Temperature

Numerical optimisation was performed in Design Expert v.12.0 to determine the configuration that gives the minimum possible temperature rise on the solar PV array as shown by Fig. 12. The input parameters used were the tilt angle and the orientation while the output parameter was the temperature rise. The optimisation revealed a tilt of 35.4219 ° and an orientation of 22.1484°. This configuration gave an average temperature of 34.1 °C and a maximum temperature of 50.376 °C. On the other hand, the average velocity experienced was 10.0603 m/s while the TKE associated with such a configuration was 0.348912 m^2/s^2. The optimisation shows that for tilt angles above 20° and orientations above 5°, there is low temperature generated and hence the optimum solution lies in this region.

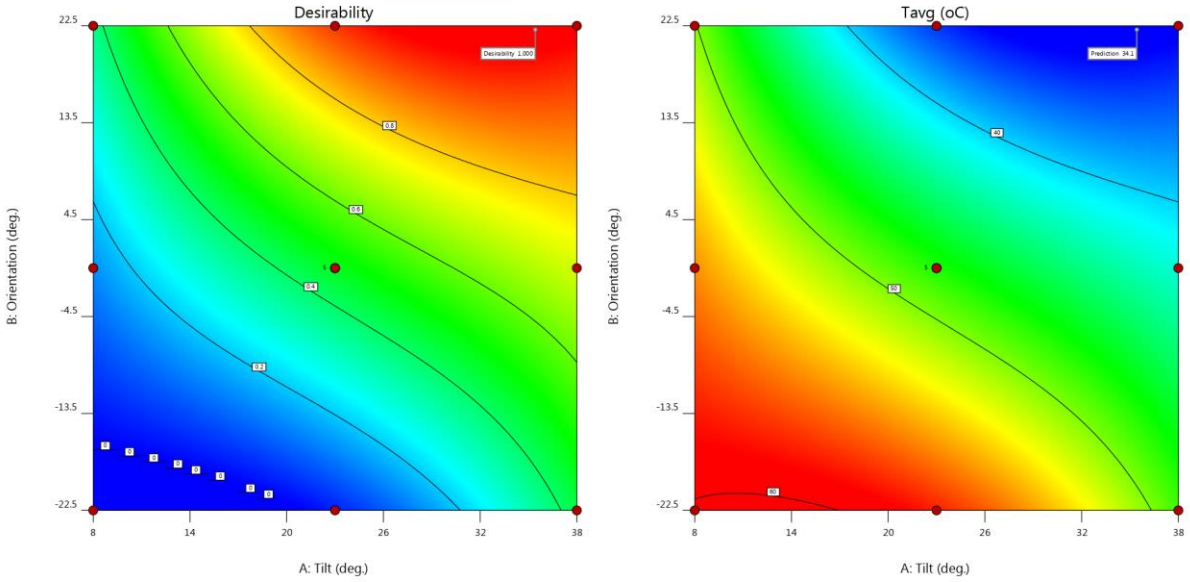

Fig. 12. Numerical optimisation of the installation configuration to minimise temperature.

Optimization for energy generation

The results from the simulation studies were used to run simulations in PVsyst to determine the annual energy generated on a hypothetical 25 kW solar PV array under different temperatures as obtained from CFD simulations as shown by Fig. 13 and 14. Different values of the thermal parameter (U) were obtained from CFD simulations and used in the PVsyst energy simulations. The values of ambient temperature and global irradiance were taken as the daily average and each day had its own values. The efficiency of the PV cells was taken as 18.9 % while the absorptivity was taken as 0.9.

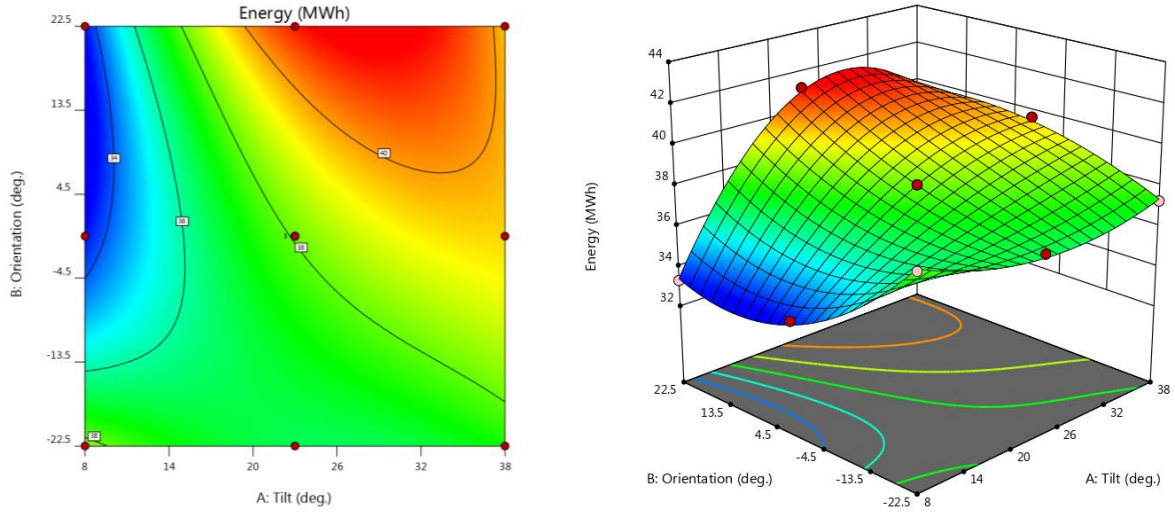

(a) (b)

Fig. 13. (a) Contours the energy generated under varying installation configurations (b) Response surface of the energy generated under varying tilt and orientation angles.

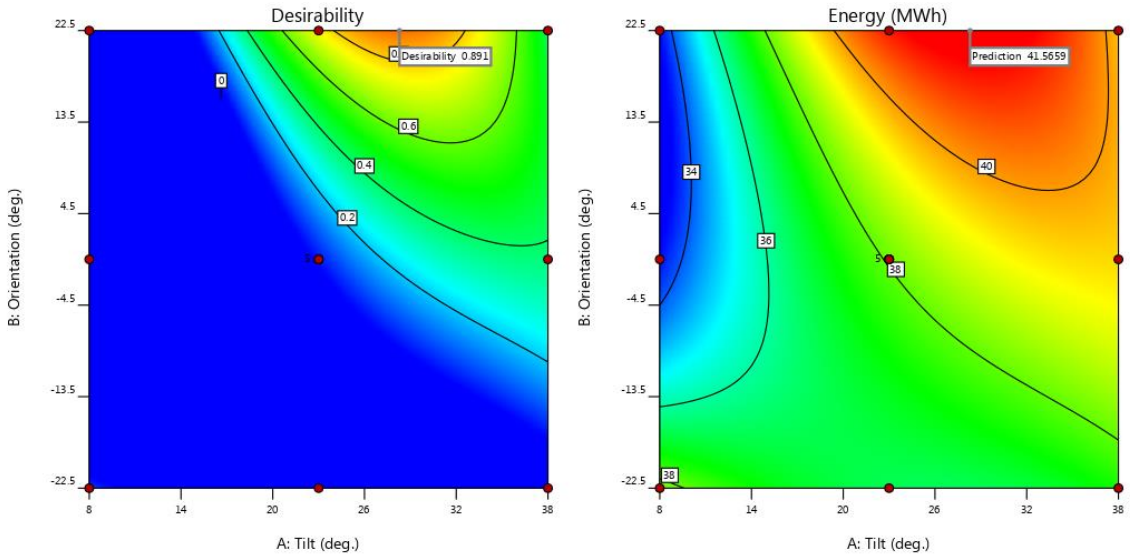

Fig. 14. Optimisation Contours

The simulations in PVsyst were used to select an optimum configuration for maximising the energy generated. The Installation configuration was optimised using the tilt, orientation and the cell temperature as the input parameters. The annual energy generated under these different parameters was taken as the output. RSM was used to optimise the configuration to select the one with the highest energy output. A quadratic polynomial was selected for the response surface generation. It is revealed that tilt angle values from 23° up to 35° combined with an orientation between 5° and 22.5° have a positive influence on energy generated. Tilt angles greater than 35° proved to be detrimental to power generation evident from the low power output. The results reveal that, as the orientation change from 5° (N) to 22.5° (NNE) there is a significant improvement in energy generated.
The optimisation of the installation configuration gives a tilt of 28.2°, orientation of 13.2° which results in 39.9 MWh of energy generated.

Energy gained due to temperature minimisation
A comparison of the energy generated with and without optimisation was performed. The comparison revealed that installation optimisation using Response Surface Optimisation results in extra 1.5MWh of energy being generated and this is equivalent to 3.9 % more energy generated. Considering a Feed-in-Tariff of US$0.15, this translates to an additional annual income of US$225 which is a revenue of US$5625 in the expected lifetime of the 25 kW solar PV plant of 25 years
The economic gain obtained from the different optimisation techniques is outlined in Table 3 where 'General' implies the generally accepted optimum configuration of 0°N and 23° tilt angle. It is shown that there is more power generated by temperature optimised configuration when compared to the general configuration. There are higher values of NPV, IRR and lower values of payback for the temperature optimised configuration.

Table 6. Comparison of the NPV, IRR and payback values of the three possible configurations

	Optimisation	NPV ($)	IRR (%)	Payback (years)
1	General	14847.07	22.06	6.8
2	RSM	18852.38	23.03	6.0

Conclusions and recommendations

The study investigated the factors contributing to temperature characteristics of a solar photovoltaic cell. Up to 14 meteorological parameters were evaluated and out of these 4 were selected for predictive model development using Artificial Neural Networks. The model developed was found to be accurate with a coefficient of determination (R^2) above 90 %. Temperature distribution experienced on the PV collectors was also investigated. The turbulent air flow characteristic behaviour on a hypothetical 25 kW solar system was analyzed using a three dimensional computational fluid dynamics model. The impact of installation azimuth and tilt as well as meteorological parameters on temperature characteristics was analyzed. Response Surface Methodology based optimization model was developed and in this study, several observations were noted as follows:

- Temperature can be accurately predicted using pressure, humidity, wind speed and direction with a coefficient of determination (R^2) above 90 %.
- The air flow velocity fields and the temperature characteristics are dependent on the installation configuration and the meteorological parameters such as wind direction and speed.
- Steep tilt angles experience higher impact wind velocities unlike less steep installation angles. Low tilt angles experience a broader spectrum of impact velocities, henceforth higher temperatures were recorded.
- Optimisation of the installation tilt was found to significantly reduce the temperature rise on the solar photovoltaic array while maximizing the energy generated by the solar photovoltaic array. The optimization performed was able to increase energy generated by 3.9 % thus increasing the total lifetime energy harvested by US$5625.
- The generally agreed tilt and orientation of 23° and 0° North are not always the best configuration for solar photovoltaic installations in Zimbabwe. A configuration of 28.2° tilt and 13.2° azimuth gave the optimum energy generated with an average annual cell temperature of 29.3 °C. This resulted in 3.9 % extra energy being generated.

Declaration of interests

The authors declare that they have no known competing financial interests or personal relationships that could have appeared to influence the work reported in this paper.

References

Ahadi A, Hayati H, Mitra J, et al (2016) A new method for estimating the longevity and degradation of photovoltaic systems considering weather states. Front Energy 10:277–285. https://doi.org/10.1007/s11708-016-0400-3

Al-Nimr MA, Kiwan S, Sharadga H (2018) Simulation of a novel hybrid solar photovoltaic/wind system to maintain the cell surface temperature and to generate electricity. International Journal of Energy Research 42:985–998. https://doi.org/10.1002/er.3885

Conceição R, Silva HG, Collares-Pereira M (2018) CSP mirror soiling characterization and modeling. Solar Energy Materials and Solar Cells 185:233–239. https://doi.org/10.1016/j.solmat.2018.05.035

Dubey S, Sarvaiya JN, Seshadri B (2013) Temperature Dependent Photovoltaic (PV) Efficiency and Its Effect on PV Production in the World – A Review. Energy Procedia 33:311–321. https://doi.org/10.1016/j.egypro.2013.05.072

Goel AK, Singh SN (2017) Thermal Performance of Solar Air Heater using Jet Impingement Technique with Longitudinal Fins. JSIR Vol76(12) [December 2017]

Goel AK, Singh SN (2019a) Performance studies of a jet plate solar air heater with longitudinal fins. International Journal of Ambient Energy 40:119–127. https://doi.org/10.1080/01430750.2017.1372808

Goel AK, Singh SN (2019b) Influence of fin density on the performance of an impinging jet with fins type solar air heater. Environment, Development and Sustainability: A Multidisciplinary Approach to the Theory and Practice of Sustainable Development 22:5873–5886
Goel AK, Singh SN (2020) Experimental study of heat transfer characteristics of an impinging jet solar air heater with fins. Environ Dev Sustain 22:3641–3653. https://doi.org/10.1007/s10668-019-00360-1
Goossens D, Lundholm R, Goverde H, Govaerts J (2019) Effect of soiling on wind-induced cooling of photovoltaic modules and consequences for electrical performance. Sustainable Energy Technologies and Assessments 34:116–125. https://doi.org/10.1016/j.seta.2019.05.007
Hartner M, Ortner A, Hiesl A, Haas R (2015) East to west – The optimal tilt angle and orientation of photovoltaic panels from an electricity system perspective. Applied Energy 160:94–107. https://doi.org/10.1016/j.apenergy.2015.08.097
Kaldellis JK, Kapsali M, Kavadias KA (2014) Temperature and wind speed impact on the efficiency of PV installations. Experience obtained from outdoor measurements in Greece. Renewable Energy 66:612–624. https://doi.org/10.1016/j.renene.2013.12.041
Kumar KA, Sundareswaran K, Venkateswaran PR (2014) Performance study on a grid connected 20kWp solar photovoltaic installation in an industry in Tiruchirappalli (India). Energy for Sustainable Development 23:294–304. https://doi.org/10.1016/j.esd.2014.10.002
Kumar NM, Yadav SK, Chopra SS, et al (2020) Operational performance of on-grid solar photovoltaic system integrated into pre-fabricated porTable cabin buildings in warm and temperate climates. Energy for Sustainable Development 57:109–118. https://doi.org/10.1016/j.esd.2020.05.008
Kumar R, Rosen MA (2011) A critical review of photovoltaic–thermal solar collectors for air heating. Applied Energy 88:3603–3614. https://doi.org/10.1016/j.apenergy.2011.04.044
Lau KY, Tan CW, Yatim AHM (2018) Effects of ambient temperatures, tilt angles, and orientations on hybrid photovoltaic/diesel systems under equatorial climates. Renewable and Sustainable Energy Reviews 81:2625–2636. https://doi.org/10.1016/j.rser.2017.06.068
Lu H, Zhao W (2019) CFD prediction of dust pollution and impact on an isolated ground-mounted solar photovoltaic system. Renewable Energy 131:829–840. https://doi.org/10.1016/j.renene.2018.07.112
Mirzaei PA, Carmeliet J (2015) Influence of the underneath cavity on buoyant-forced cooling of the integrated photovoltaic panels in building roof: a thermography study. Progress in Photovoltaics: Research and Applications 23:19–29. https://doi.org/10.1002/pip.2390
Mirzaei PA, Paterna E, Carmeliet J (2014) Investigation of the role of cavity airflow on the performance of building-integrated photovoltaic panels. Solar Energy 107:510–522. https://doi.org/10.1016/j.solener.2014.05.003
Proposal a PD (2011) Experimental Investigations of Wind Effect on Solar Panels Ayodeji Abiola-Ogedengbe
Siecker J, Kusakana K, Numbi BP (2017) A review of solar photovoltaic systems cooling technologies. Renewable and Sustainable Energy Reviews 79:192–203. https://doi.org/10.1016/j.rser.2017.05.053
Tominaga Y, Akabayashi S ichi, Kitahara T, Arinami Y (2015) Air flow around isolated gable-roof buildings with different roof pitches: Wind tunnel experiments and CFD simulations. Building and Environment 84:204–213. https://doi.org/10.1016/j.buildenv.2014.11.012
Vafaei S, Rezvani A, Gandomkar M, Izadbakhsh M (2015) Enhancement of grid-connected photovoltaic system using ANFIS-GA under different circumstances. Front Energy 9:322–334. https://doi.org/10.1007/s11708-015-0362-x
Wole-Osho I, Adun H, Adedeji M, et al (2020) Effect of hybrid nanofluids mixture ratio on the performance of a photovoltaic thermal collector. International Journal of Energy Research n/a: https://doi.org/10.1002/er.5619

Yadav SK, Bajpai U (2018) Performance evaluation of a rooftop solar photovoltaic power plant in Northern India. Energy for Sustainable Development 43:130–138. https://doi.org/10.1016/j.esd.2018.01.006
Zhang R, Mirzaei PA, Carmeliet J (2017) Prediction of the surface temperature of building-integrated photovoltaics: Development of a high accuracy correlation using computational fluid dynamics. Solar Energy 147:151–163. https://doi.org/10.1016/j.solener.2017.03.023
(2013) ANSYS Fluent Theory Guide. 15317:724–746

Figures

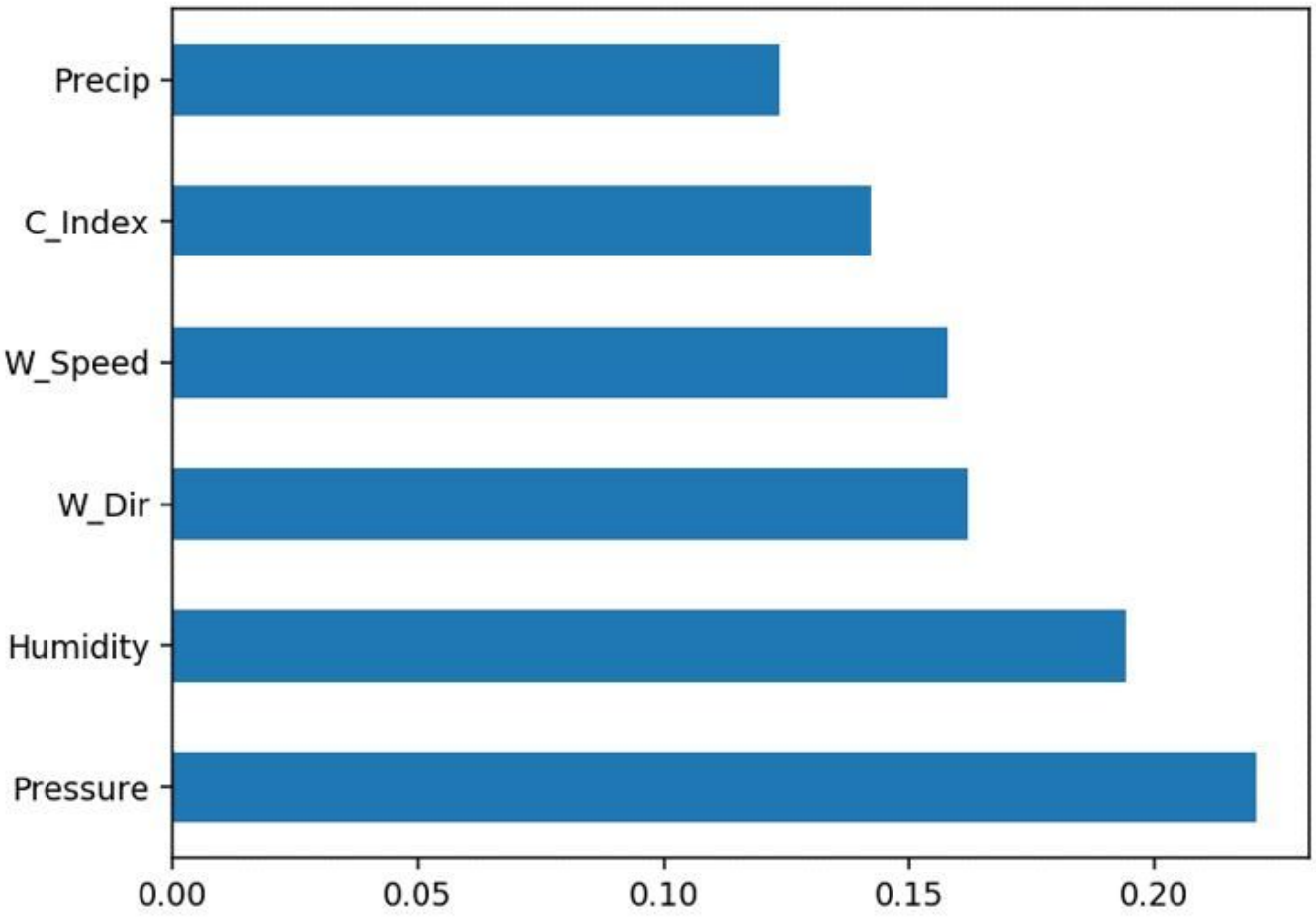

Figure 1

Parameter correlation analysis using Boruta algorithm.

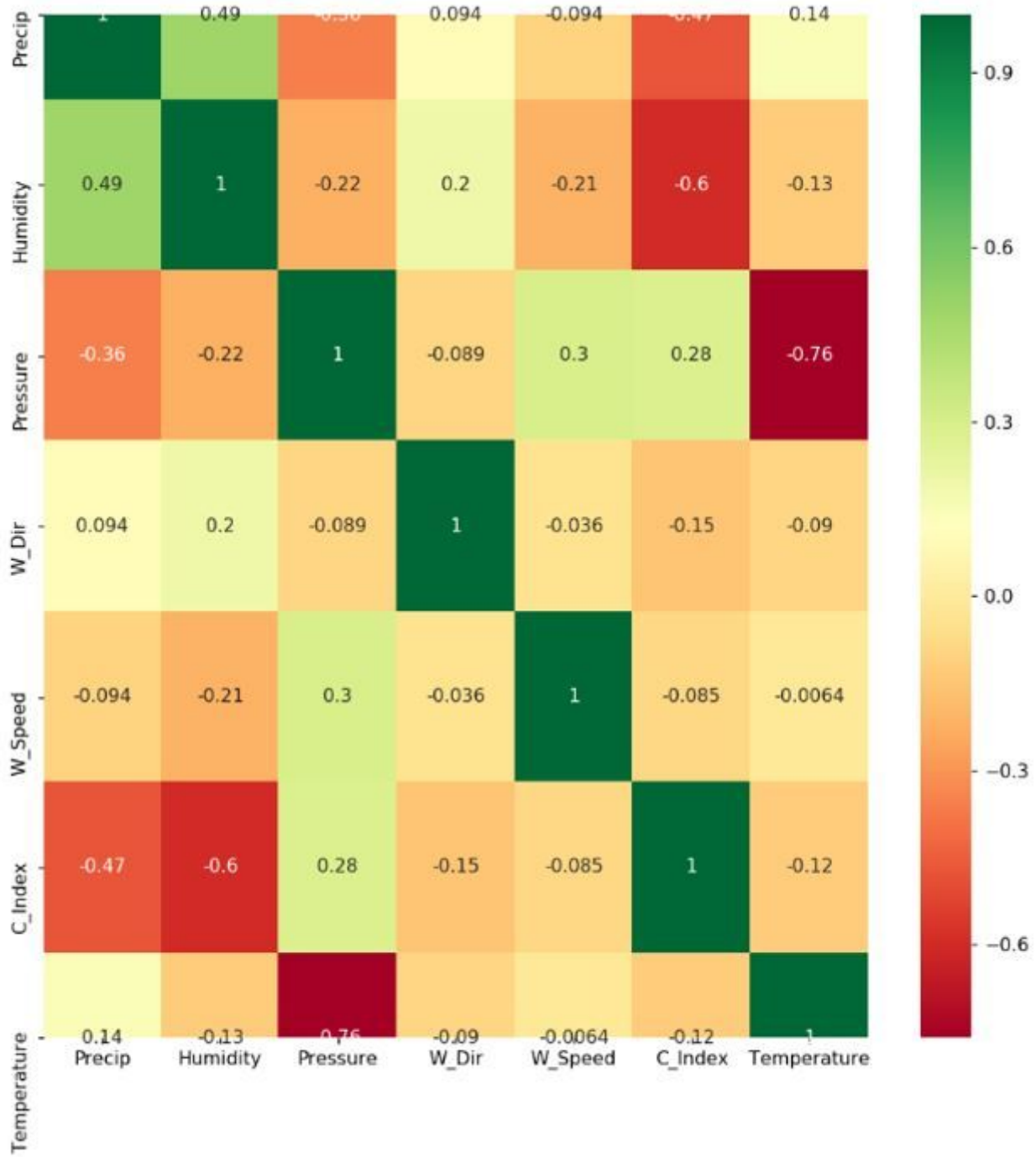

Figure 2

Correlation matrix for variable selection

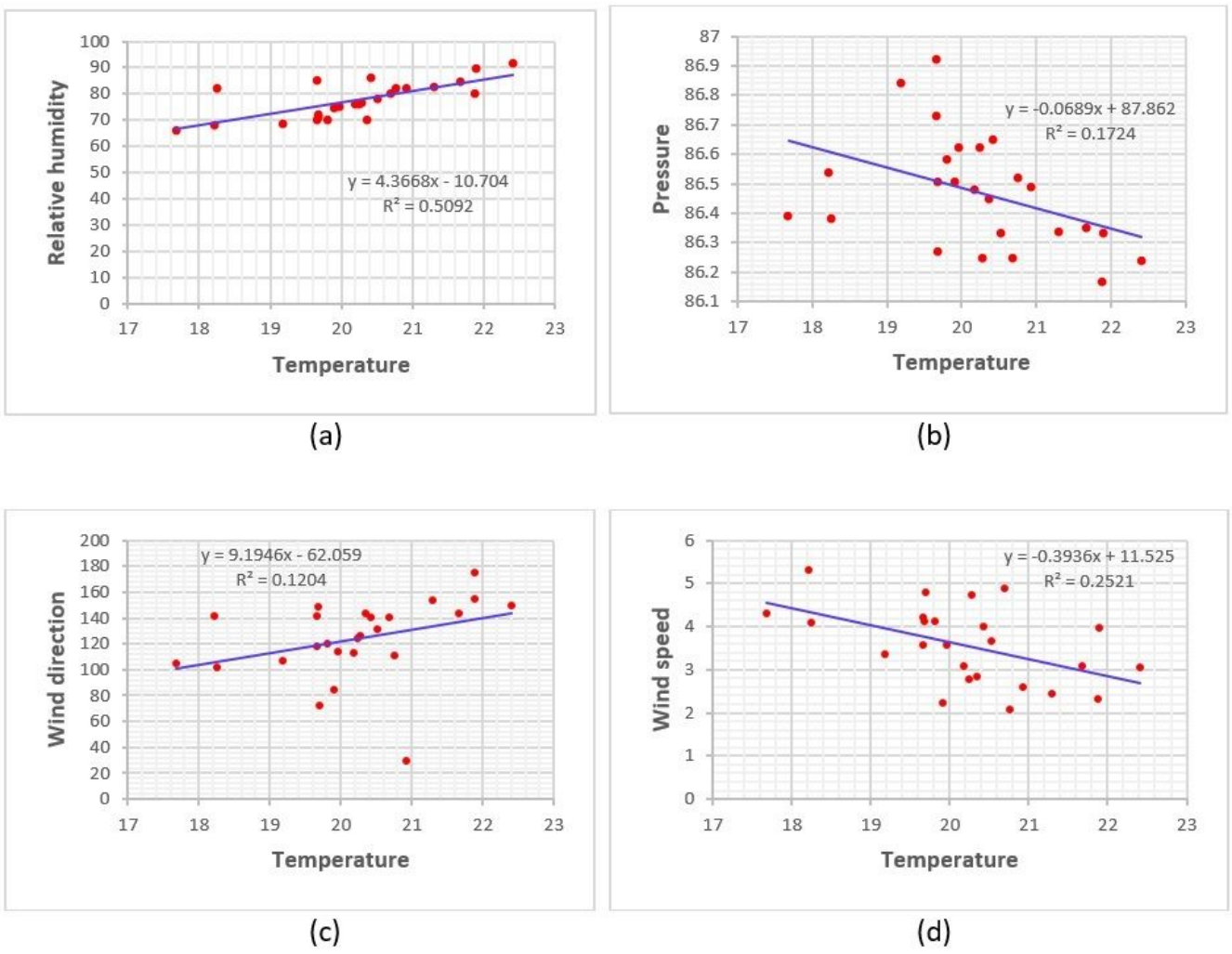

Figure 3

Correlation of temperature with; relative humidity (a), pressure (b), wind direction (c) and wind speed (d).

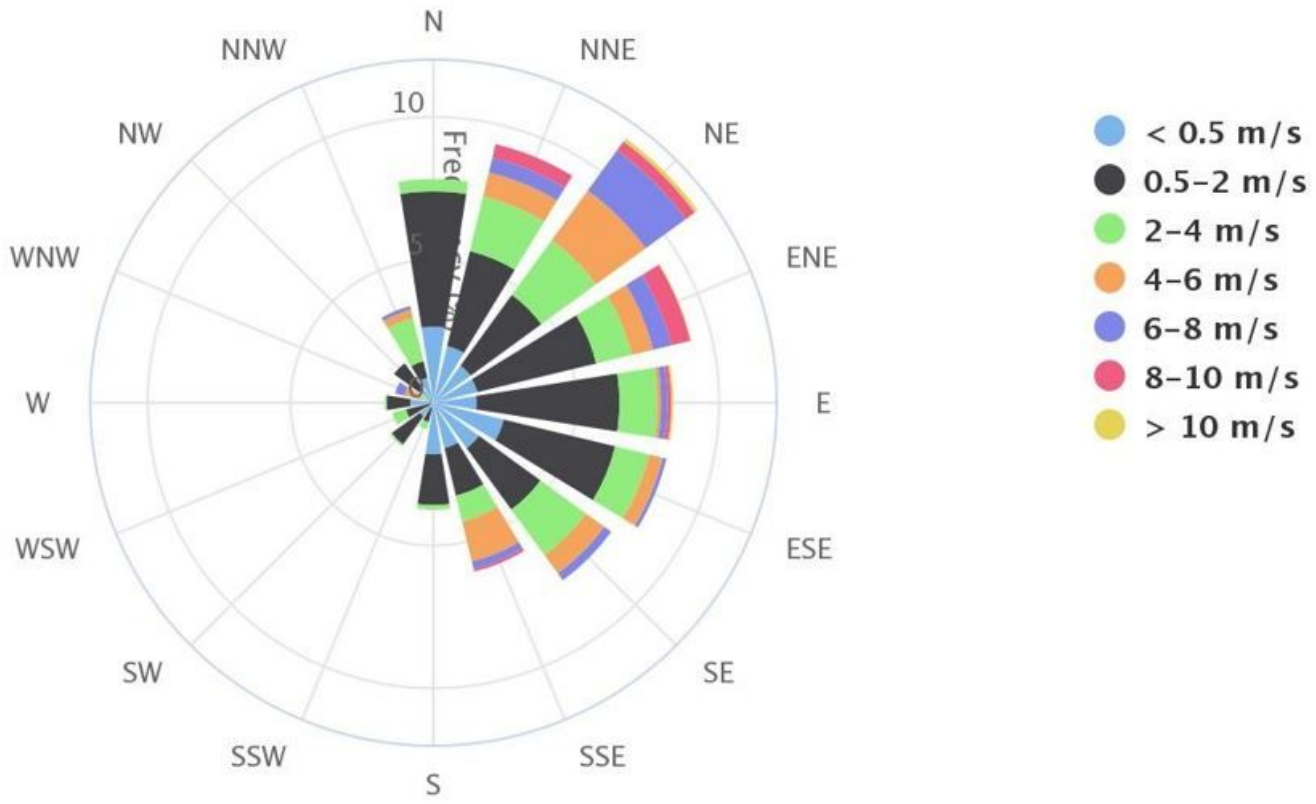

Figure 4

Wind Rose showing the 10 year annual average wind speed and direction

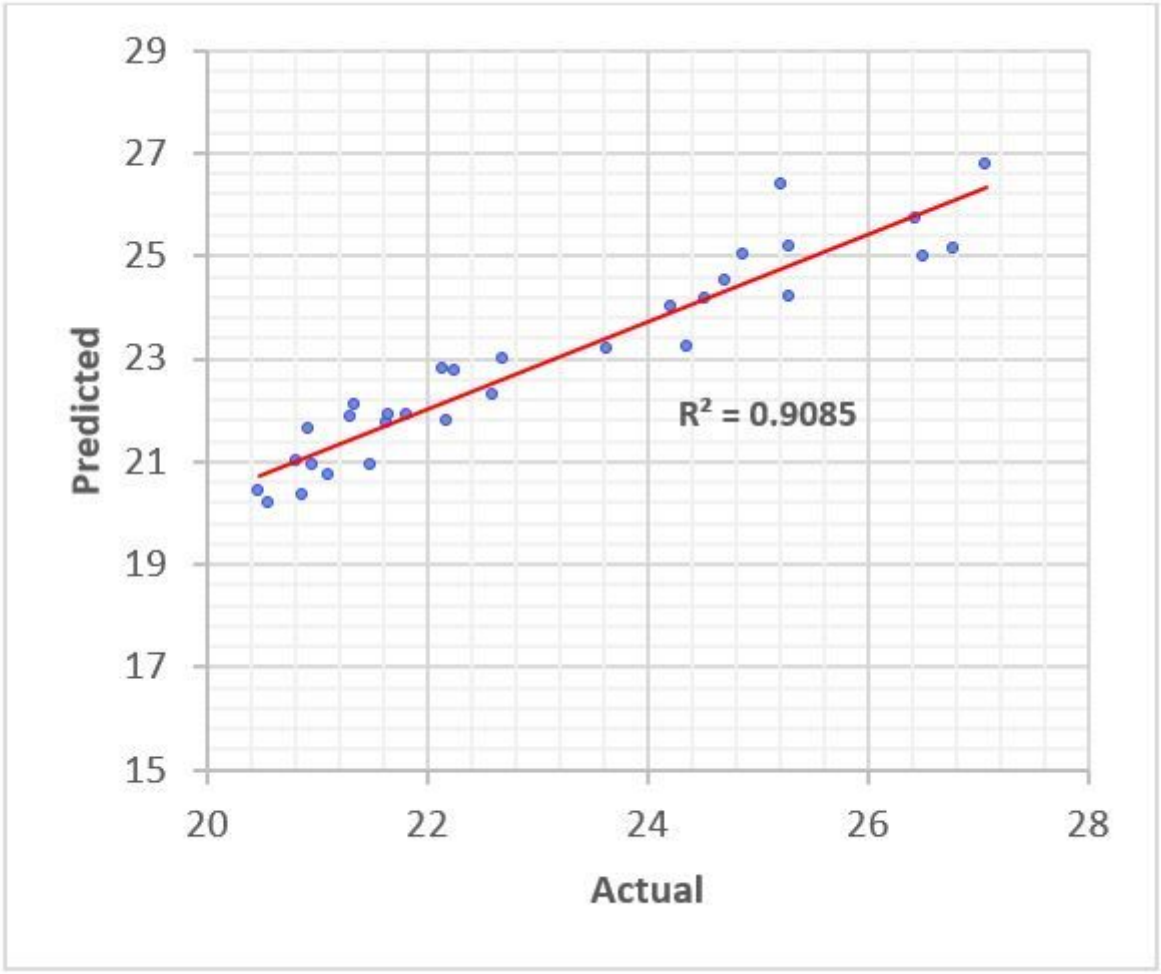

Figure 5

ANN model validation

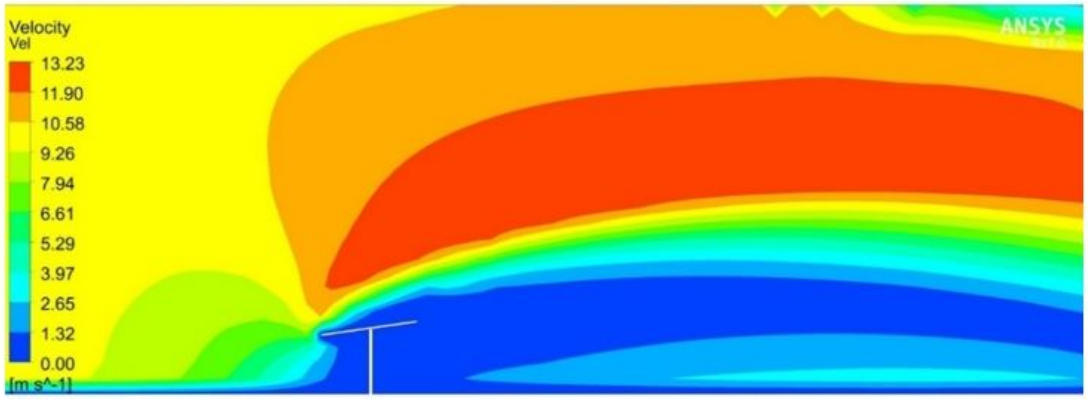

(a) 8° tilt

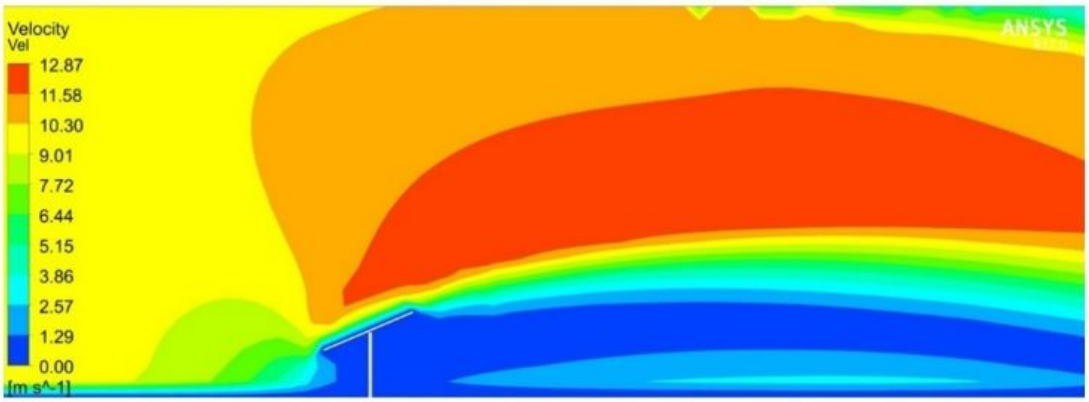

(b) 23° tilt

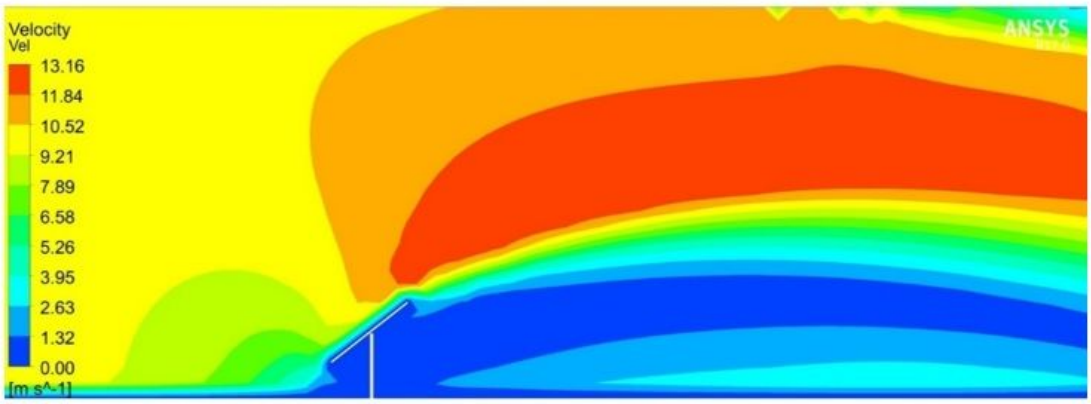

(c) 38° tilt

Figure 6

Velocity profiles

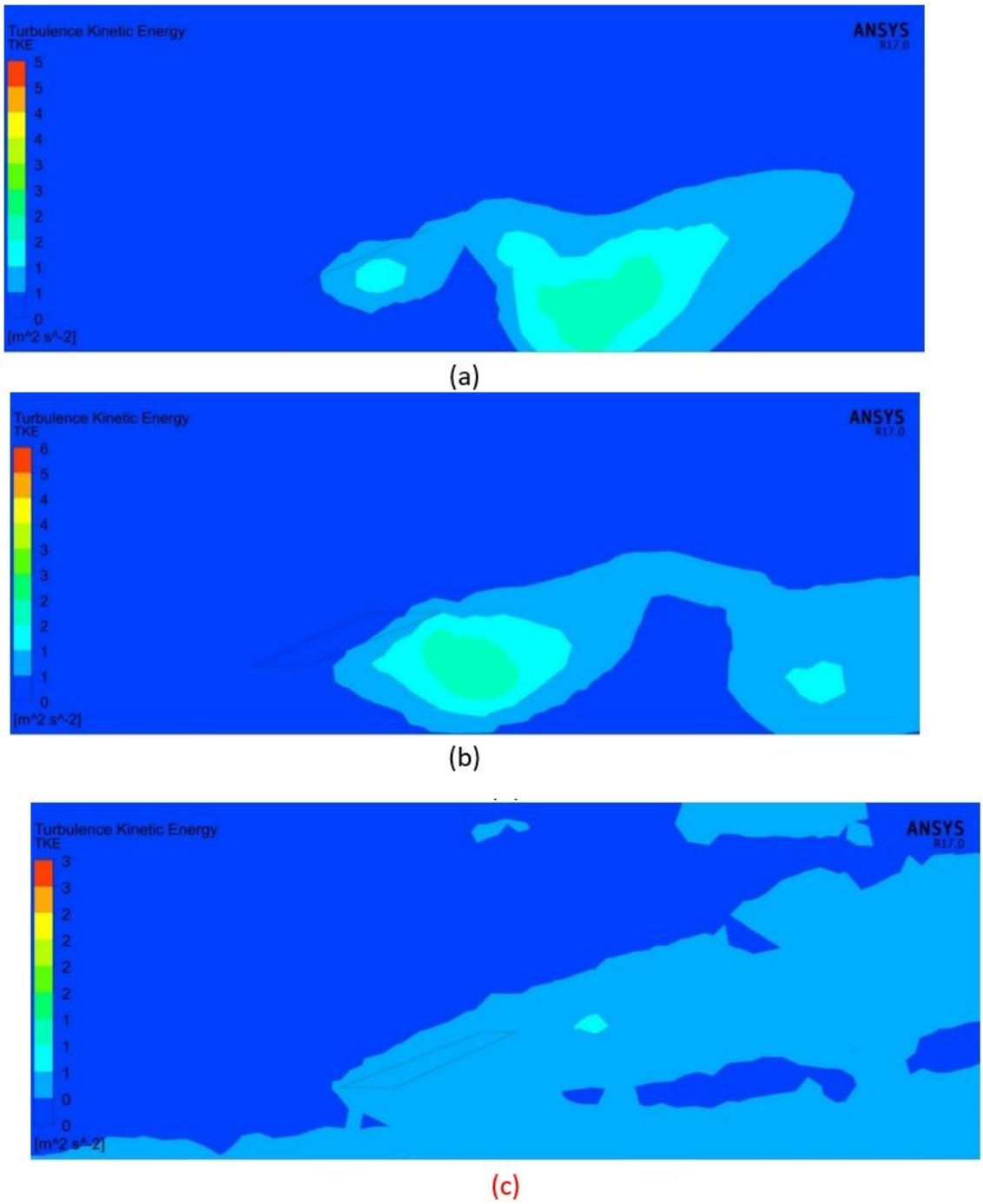

Figure 7

TKE Profiles at 23o tilt; (a) 0o orientation, (b) 22.5o orientation, (c) -22.5o orientation

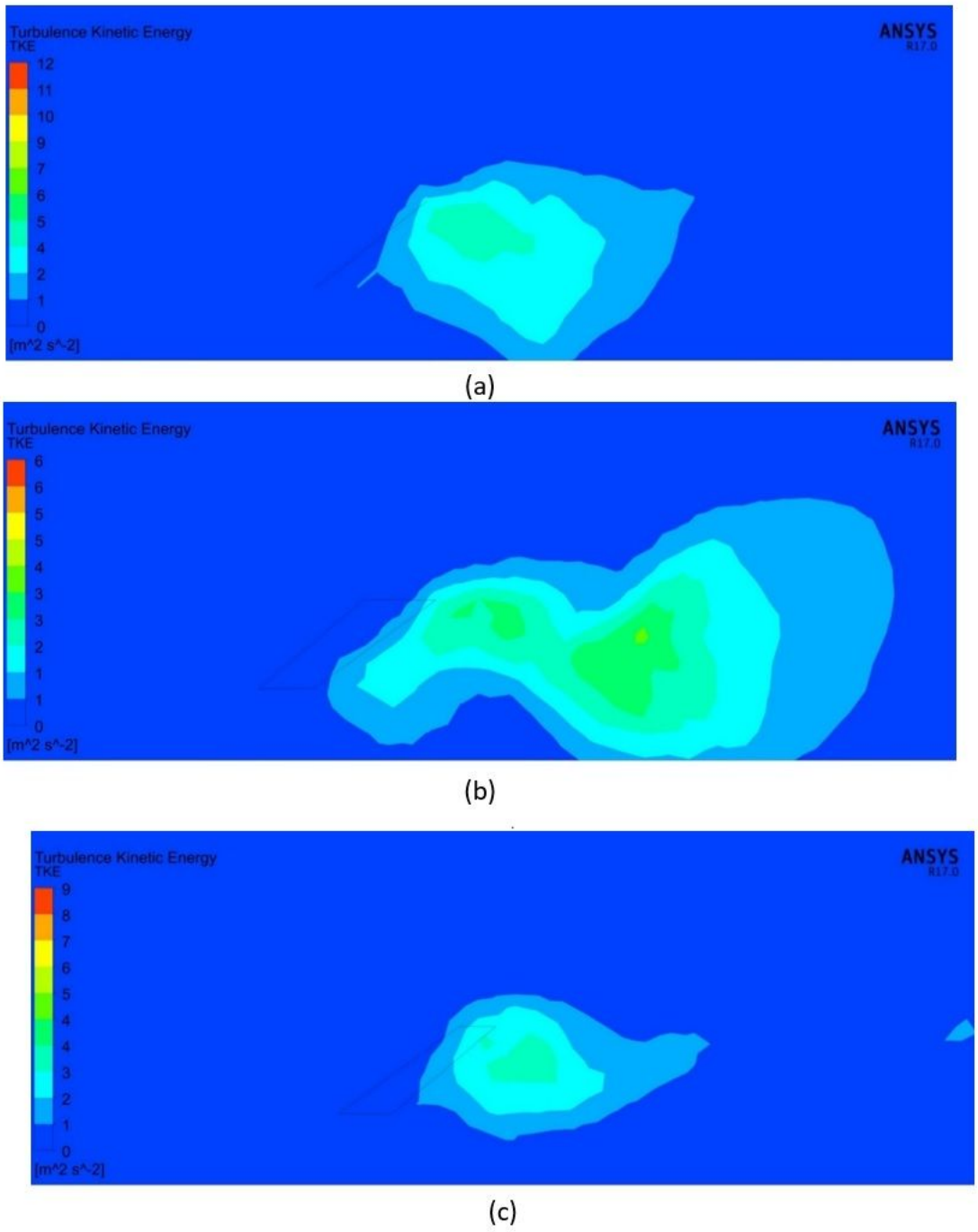

Figure 8

TKE Profiles at 38o tilt; (a) 0o orientation, (b) 22.5o orientation, (c) -22.5o orientation

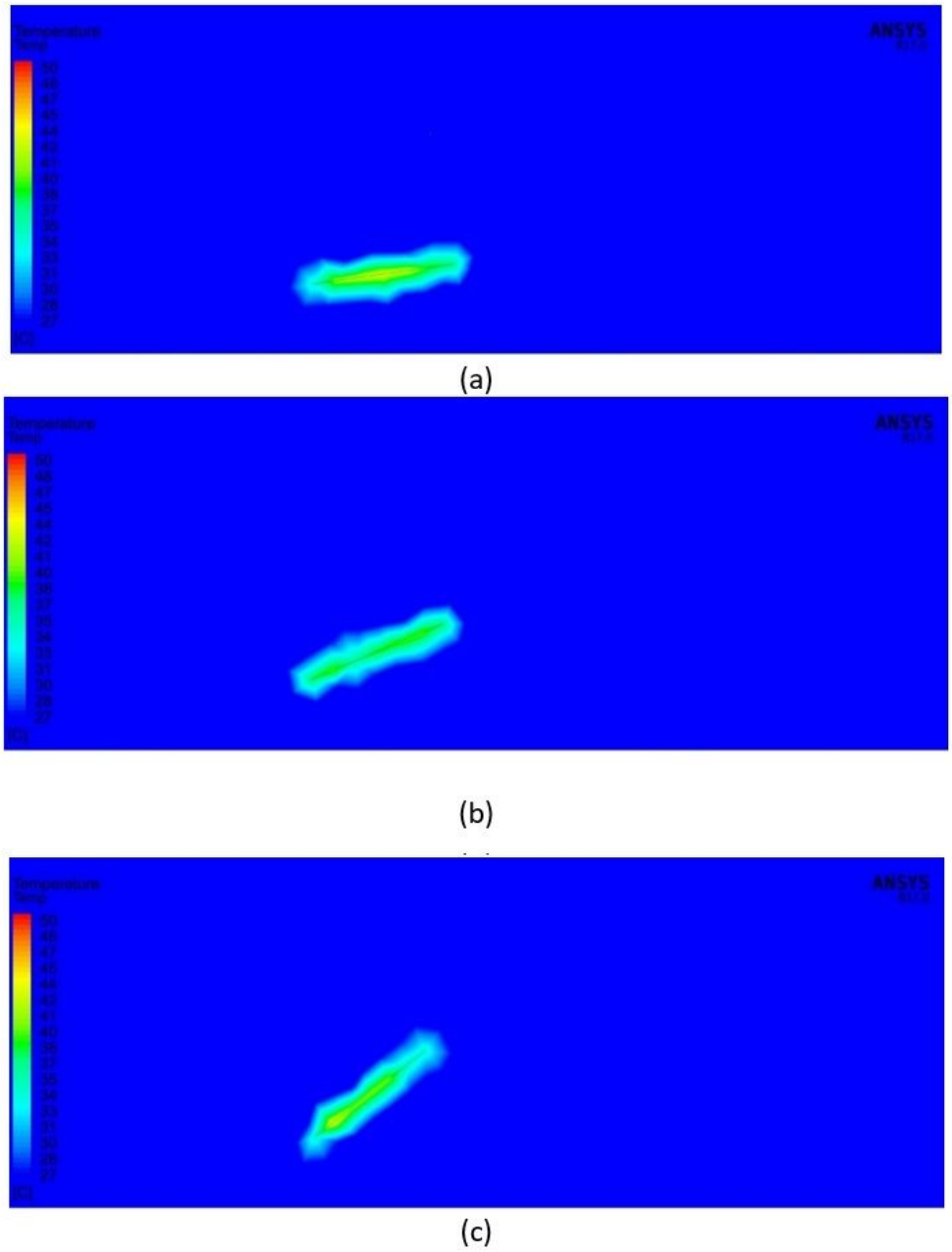

Figure 9

Temperature profiles at 0o orientation; (a) 8o tilt, (b) 23o tilt (c) 38o tilt

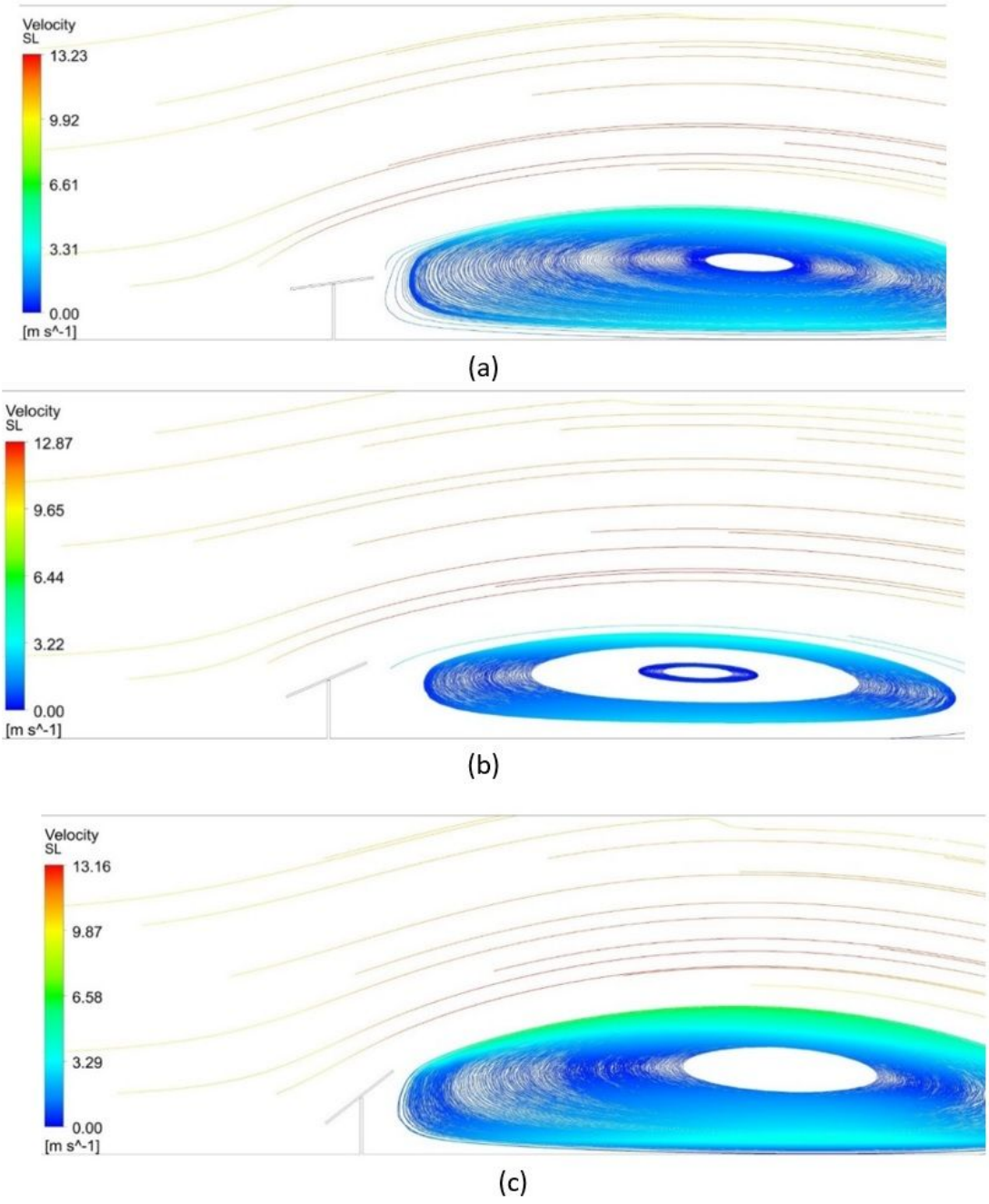

Figure 10

Velocity streamlines at tilt degrees of (a) 8o (b) 23o and (c) 38o

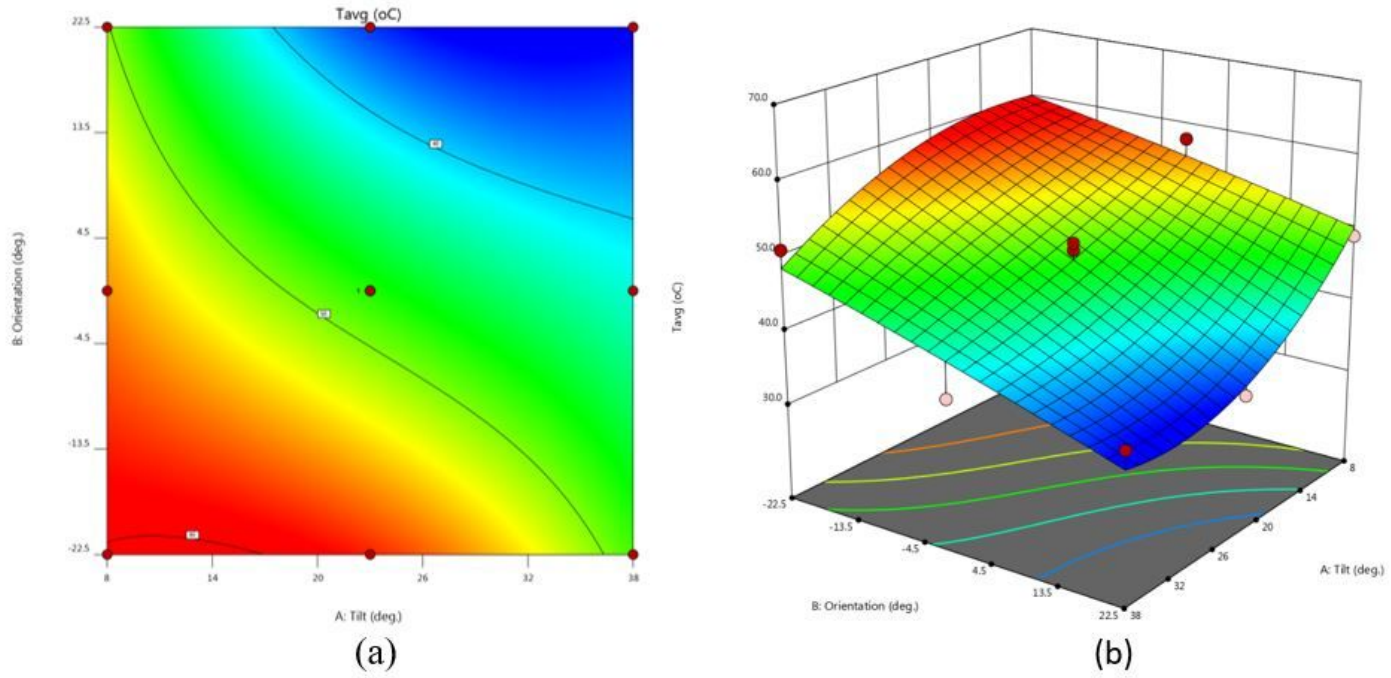

Figure 11

Average temperature contours Response surface for the average temperature.

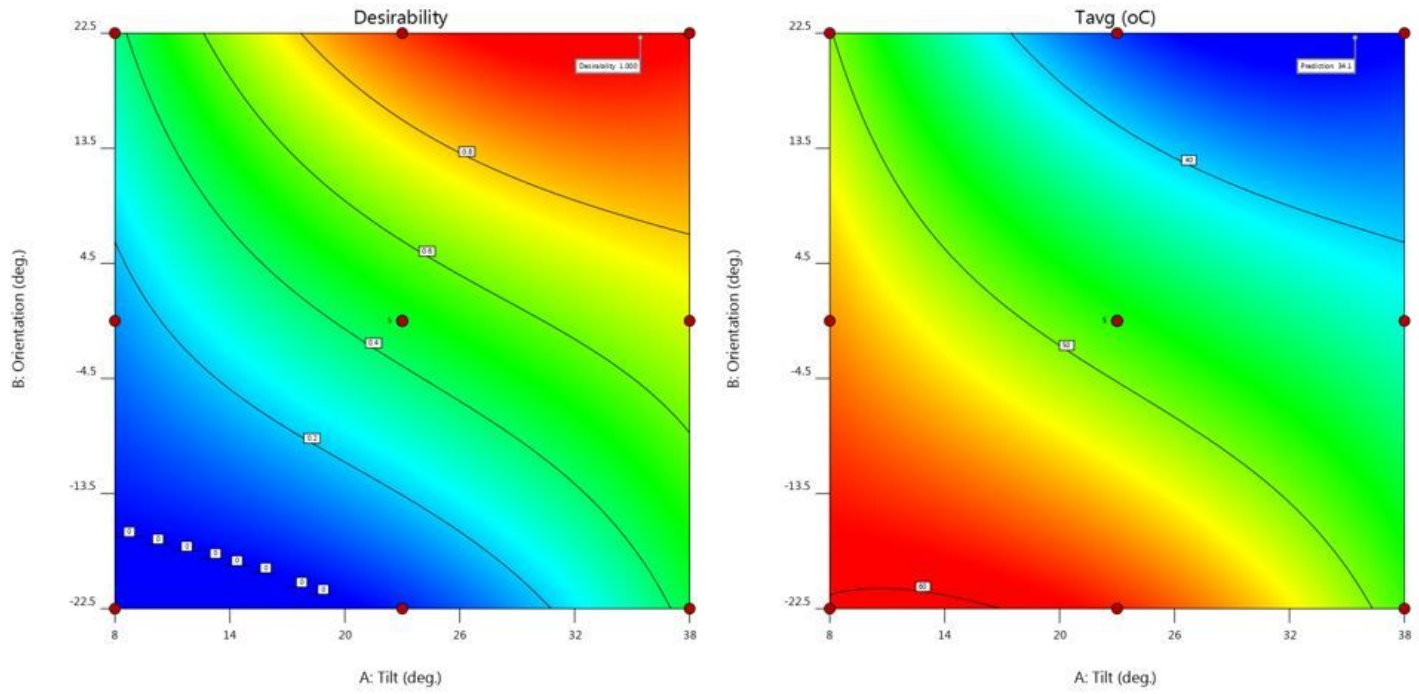

Figure 12

Numerical optimisation of the installation configuration to minimise temperature.

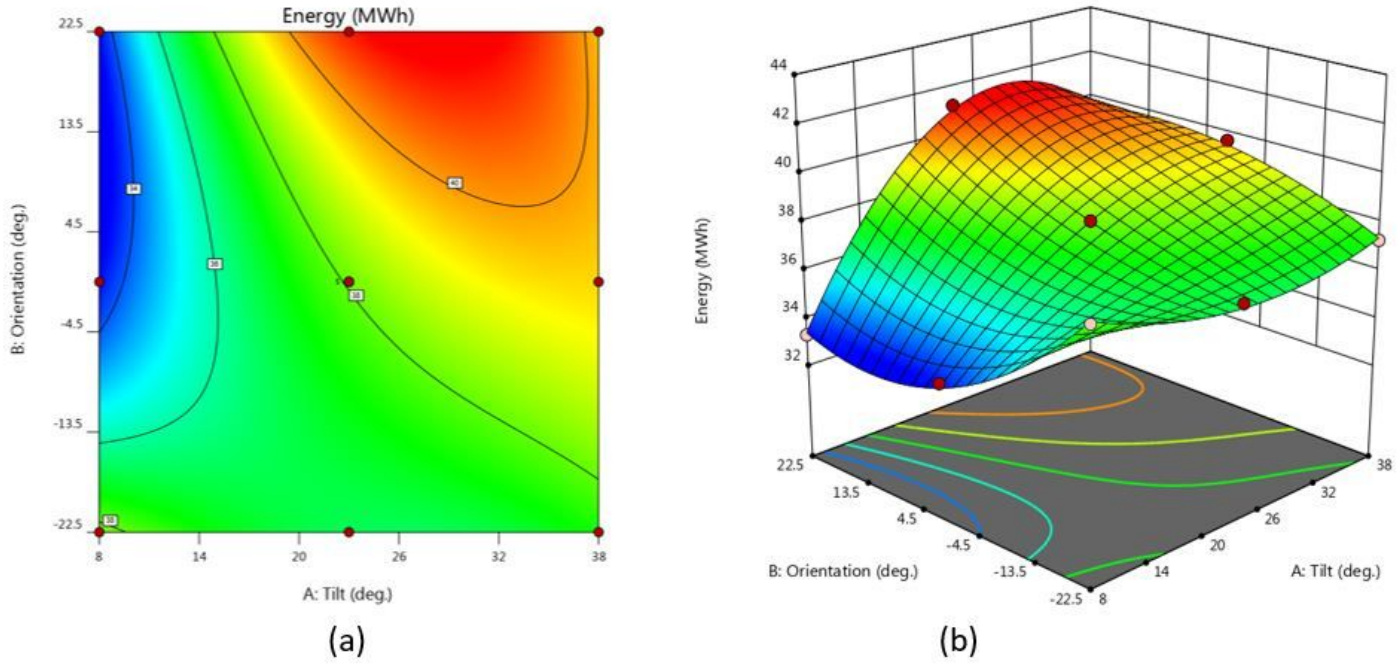

Figure 13

(a) Contours the energy generated under varying installation configurations (b) Response surface of the energy generated under varying tilt and orientation angles.

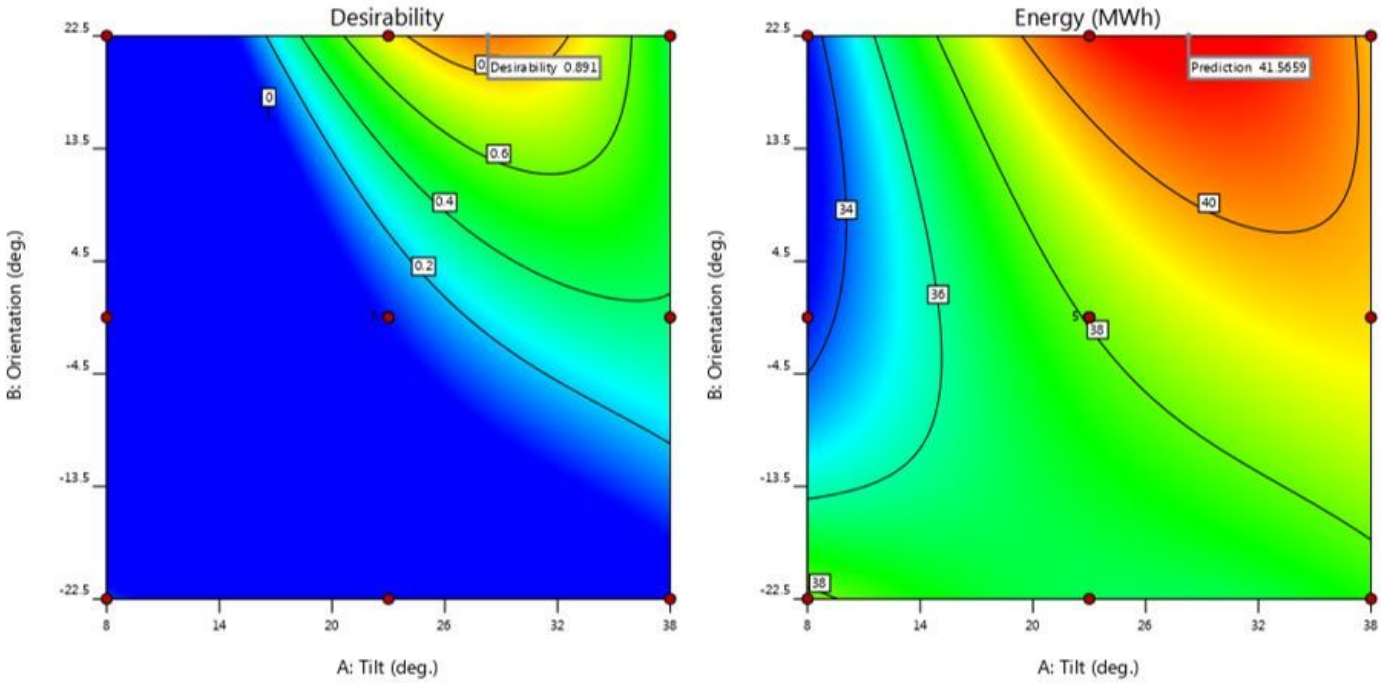

Figure 14

Optimisation Contours

Supplementary Files

This is a list of supplementary files associated with this preprint. Click to download.

- GraphicalAbstract.docx